Supporting Information

Controlling optoelectronic properties through protonation with π-extended triphenodioxazine diimides

Rhea Kumar,[a] Mario Taddei,[f] Vasilis Petropoulos,[a] Mattia Russo,[a] Federico Vernuccio,[a] Giulio Cerullo,[a] Dario Polli,[a] Artur Nenov,[f] Nicola Demitri,[e] Maurizio Prato,[*b,c,d] Margherita Maiuri[*a] and Jacopo Dosso[*b]

a) Department of Physics, Politecnico di Milano, Piazza Leonardo da Vinci 32, 20133 Milano, Italy.
b) Department of Chemical and Pharmaceutical Sciences, CENMAT, Centre of Excellence for Nanostructured Materials, INSTM UdR Trieste, University of Trieste, via Licio Giorgieri 1, 34127 Trieste, Italy.
c) Centre for Cooperative Research in Biomaterials (CIC BiomaGUNE), Basque Research and Technology Alliance (BRTA), Paseo de Miramón 194, 20014, Donostia San Sebastián, Spain
d) Basque Fdn Sci, Ikerbasque, 48013 Bilbao, Spain.
e) Elettra—Sincrotrone, Trieste S.S. 14 Km 163.5, Area Science Park, 34149 Basovizza, Trieste (Italy)
f) Department of industrial chemistry, University of Bologna, Viale del Risorgimento, 40136 Bologna, Italy

Summary

1. General Remarks 2
1.1 Instrumentation 2
1.2 Materials and synthetic methods 4
1.3 Time-resolved spectroscopic methods 4
2 Synthetic procedures and spectral data 6
2.1 Synthesis of 3 6
2.2 Synthesis of 4 6
2.3 Synthesis of 5 7
2.4 Synthesis of 1 8
2.5 Synthesis of 7 9
2.6 Synthesis of 8 9
2.7 Synthesis of 9 10
2.8 Synthesis of 10 10
2.9 Synthesis of 1Br 11
3 NMR and HRMS spectra 12
3.1 Characterization of 3 12
3.2 Characterization of 4 13
3.3 Characterization of 5 15
3.4 Characterization of 1 16
3.5 Characterization of 7 20
3.6 Characterization of 8 21
3.7 Characterization of 9 22
3.8 Characterization of 10 24

4 UV-Vis and electrochemistry studies 25
5 Cyclic Voltammetry studies 28
6 Computational, Raman and two-dimensional electronic spectra 29
7 X-Ray diffraction 40

1. General Remarks

1.1 Instrumentation

Thin layer chromatography (TLC) was conducted on Sigma Aldrich pre-coated aluminum sheets (0.25 mm layer thickness, 60 Å porosity and fluorescent indicator GF254) and were visualized using 254 or 365 nm light. Flash column chromatography was carried out using Merck Gerduran silica gel 60 (particle size 40 63 μm). ***Melting points*** (M.P.) were measured on a Gallenkamp apparatus. All melting points have been measured in open capillary tubes and have not been corrected. ***Nuclear magnetic resonance*** (NMR) ^{1}H, and ^{13}C spectra were obtained on Varian Inova spectrometer (500 MHz ^{1}H and 126 MHz ^{13}C) or Varian 400 MHz NMR spectrometer (400 MHz ^{1}H and 101 MHz ^{13}C). Chemical shifts were reported in ppm according to tetramethylsilane using the solvent residual signal as an internal reference ($CDCl_3$: δ_H = 7.26 ppm, δ_C = 77.16 ppm, CD_2Cl_2: δ_H = 5.32 ppm, δ_C = 53.84 ppm, TFA-*d*1: δ_H = 11.50 ppm, δ_C = 164.20, 116.60 ppm). Coupling constants (*J*) were given in Hz. Resonance multiplicity was described as s (singlet), d (doublet), t (triplet), m (multiplet), br (broad signal), dd (doublet of doublets), dt (doublet of triplets). Carbon spectra were acquired with a complete decoupling for the proton, unless specified. All spectra were recorded at 25 °C unless specified. ***Infrared spectra*** (IR) were recorded on a Shimadzu IR Affinity 1S FTIR spectrometer in ATR mode with a diamond mono-crystal. Selected absorption bands are reported in wavenumber (cm^{-1}). ***Coherent Anti-Stokes Raman Scattering (CARS) spectra*** were recorded using a home-built setup that has been described in detail previously.[1] Briefly, the system started with an amplified ytterbium fiber laser (Coherent Monaco) generating pulses (270 fs, 1035 nm) which split into two beams using a beam splitter. One portion of the beam was used to generate pump pulses (3.7 ps, 1035 nm) using an optimized etalon achieving spectral resolution of < 9 cm^{-1} FWHM. The other portion of the beam was focused into a 10 mm thick Yttrium Aluminium Garnett (YAG) crystal to generate a white light continuum, from which the residual fundamental was filtered out using a long-pass filter. The Stokes pulses were then compressed to ~20 fs using a SF_{11} prism-pair compressor. The pump and Stokes beams were combined and focused onto the sample and the resulting spectra were recorded using a spectrometer, composed of a monochromator equipped with a CCD camera. By utilising CARS Spectroscopy, we detected the blue-shifted component of the spectrum thus avoiding the problematic high fluorescence signal, which renders the vibrational spectra for the studied systems impossible to measure by the Spontaneous Raman Spectroscopy technique. The CARS spectra shown in Fig. S41 were obtained by averaging 100 spectra acquired with 5 ms spectrum dwell time. After acquisition, we removed the non-resonant background, deriving from four-wave mixing processes, through the time-domain Kramers-Kronig algorithm.[2]

ESI-High resolution mass spectrometry (ESI-HRMS). ESI-HRMS was performed at University of Trieste Chemistry department, High resolution mass spectra (HRMS) were obtained on Bruker micrOTOF-Q (ESI-TOF). Low resolution mass spectra (LRMS) were obtained on Bruker Esquire 4000 (ESI). ***Photophysical analysis***: Absorption spectra of compounds were recorded on air equilibrated solutions at room temperature with an Agilent Cary 5000 UV-Vis-NIR double beam spectrophotometer, using quartz cells with path length of 1.0 cm. Emission measurements were performed on an Edinburgh instruments FS5 spectrofluorometer using a 150 W CW Ozone-free xenon arc lamp as source and a Photomultiplier R928P (spectral coverage 200 nm – 900 nm, cooled and stabilised) as detector. Quantum yields were performed using the integrating sphere setup SC-30 on a sample solution in a quartz cuvette and using the same solvent in another cuvette as reference. Fluorescence decay dynamics studies have been performed using 635 nm laser pulses on a FLS1000 by Edinburgh Instruments equipped with a PMT-980 detector. 10 mm path length Hellma Analytics sealable quartz cuvettes have been used. **Cyclic Voltammetry (CV**) The electrochemical characterizations were carried out in CH_2Cl_2/0.1 M tetrabutylammonium hexafluorophosphate ($TBAPF_6$), at room temperature, on an Autolab 302 N electrochemical workstation (Metrohm, The Netherlands) in a glass cell from CH Instruments (10 mL, CHI220). A typical three-electrode cell was employed, which was composed of glassy carbon (GC) working electrode (3 mm diameter), a platinum wire as counter electrode and a saturated calomel electrode (SCE) as reference electrode (RE). Oxygen was removed by purging the CH_2Cl_2 solution with Argon. The GC electrode was polished twice before use with 0.05 and 0.1 colloidal silica polishing suspension, Pt counter electrode was polished on a flame to remove organic materials. HOMO and LUMO values were obtained by converting potentials vs SCE to vs Fc/Fc^+ using a CV measurement performed in the same conditions on Fc and by applying the following formula: E HOMO = -(4.8 eV + E_{1ox} vs. Fc^+/Fc) E LUMO = -(4.8 eV + E_{1red} vs. Fc^+/Fc). In the cases where oxidation waves were not detected by means of cyclic voltammetry, HOMO levels were calculated using the optical gap E_{00}, following equation: E_{00}(eV) = 1240 (eV·nm) / λmax, rel (nm). ***X-Ray Data***: CCDC **2383224**, **2383220**, **2383219**, **2383221**, **2383222** and **2383223** contain the supplementary crystallographic data for **1** at 100K, **1** at 298K, **1Br** at 100K, **1•TFA** polymorph α at 100K, **1•TFA** polymorph α at 298K and **1•TFA** polymorph β at 100K, respectively. Related files can be obtained free of charge from The Cambridge Crystallographic Data Centre via https://www.ccdc.cam.ac.uk/structures.

1.2 Materials and synthetic methods

Chemicals were purchased from Sigma Aldrich, TCI, Alfa Aesar and Fluorochem and were used as received unless otherwise stated. Solvents were purchased from Sigma Aldrich and Alfa Aesar, while deuterated solvents from Eurisotop and Sigma Aldrich. Anhydrous conditions were achieved by repeated cycles of flaming with a heat gun under vacuum and purging with Argon (Ar). The inert atmosphere was maintained using Argon-filled balloons equipped with a syringe and needle that was used to penetrate the silicon stoppers used to close the flask's necks. Additions of liquid reagents were performed using plastic syringes. Degassing of solutions was performed by bubbling argon in the reaction under sonication for at least 10 minutes. Dry solvents were obtained commercially or via treatment on activated molecular sieves (MS, 3Å for CH_3CN).

Activation of MS was carried out by multiple cycles of heating under vacuum and the solvents were left over MS for at least 24 h. MilliQ water was obtained from a Millipore Milli-Q Plus 185 apparatus and presented a resistivity of 18.2 MΩcm. MilliQ water was always used unless otherwise specified. Derivative **2** was synthesised according to a previously reported synthesis.[3] Microwave syntheses were performed on a CEM Discover-SP, using 10 mL glass microwave vials.

1.3 Time-resolved spectroscopic methods

Transient absorption spectroscopy. A Ti:Sapphire regenerative amplifier (Libra, Coherent) generated pulses (100 fs, 800 nm, 1 kHz) which seeded a non-collinear optical parametric amplifier (NOPA) to yield a broadband pulse spectrum (530-750 nm) with < 0.5 % RMS fluctuations. The NOPA output pulses were compressed to sub-20 fs duration using a pair of chirped mirrors and the beam was split by a beamsplitter to generate separate pump and probe beams. Transient experiments were performed with perpendicular polarisation of pump and probe to minimise scattering of the pump beam. Pump and probe beams were focused onto a spot on the sample of diameters of 230 μm and 90 μm, respectively. A mechanical delay stage controlled the time delay between the pump and probe pulses; the pump-probe delay was scanned in 5 fs steps up to 1 ps. The pump beam was modulated at 500 Hz by a mechanical chopper to collect both pump-on and pump-off spectra such that difference spectra were recorded to observe only the pump-excited signals. Solutions of the sample were prepared in dichloromethane at concentrations of OD=0.5 and were measured in a 0.2 mm cuvette.

Two-dimensional electronic spectroscopy (2DES). The TA setup can be easily converted into a 2DES setup working int a pump-probe geometry and it is described in detail elsewhere).[4] Briefly, the same NOPA pulses pumped by the Ti:Sappihre laser were used for the 2DES measurements. The NOPA pulses were compressed down to sub-15 fs by a chirped mirror pair and then split into two separate pump and probe beams. The pump beam was used to generate a pair of phase-locked pump pulses using a Translating Wedge-based Identical Pulse Encoding System (TWINS), where translation of a set of birefringent α–barium borate (α–BBO) wedges controlled the time delay, t_1, between the two pulses. 2DES experiments were performed with perpendicular polarisation of the two pump pulses relative to the probe to minimise scattering of the pump beam. Pump and probe beams were focused onto a spot on the sample of diameters of 230 μm and 90 μm, respectively. A mechanical delay stage controlled the time delay, t_2, between the pump and probe pulses; the pump-probe delay was scanned in 5 fs steps up to 1 ps. The pump pulses were modulated at 500 Hz to collect both pump-on and pump-off spectra such that difference spectra were recorded to observe only the pump-excited signals. A second beamsplitter divided a portion of the pump beam to be measured using a photodiode in order to calibrate the t_1 delay. Solutions of the sample were prepared in dichloromethane at concentrations of OD=0.5 and were measured in a 0.2 mm cuvette. The kinetic traces for a particular electronic transition are extracted from 2D maps at different t_2 times for given excitation/detection wavelength. Progression of the vibrational

wavepacket gives rise to oscillations in the 2D signal in the time domain, with frequencies that correspond to the frequency of the vibrational modes. Therefore, projection of the t_2 time domain data onto the frequency domain by the Fourier Transform yields a frequency-resolved spectrum of the vibrational modes coupled to the given electronic transition.

2 Synthetic procedures and spectral data

2.1 Synthesis of 3

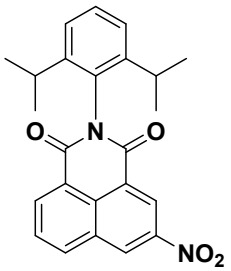

In a round bottom flask, 2-nitronaphthalene-1,3-monoanydride **2** (1.5 g, 6.2 mmol) was added and suspended in AcOH (25 mL). 2,6-diisopropyl aniline (1.4 mL, 7.4 mmol) was then added, and the resulting suspension heated at 110°C for 18 h. The brown solution was then allowed to cool to r.t., dropped in H_2O and filtered followed by washing with small amounts of cold MeOH and Et_2O to give **3** as a beige solid (1.98 g, 80%). Further purification to remove the 1-NO_2 isomer can be achieved by crystallization from EtOH.

M.P.:246-247 °C. ^{1}H NMR (400 MHz, $CDCl_3$) δ 9.37 (d, *J* = 2.2 Hz, 1 H), 9.22 (d, *J* = 2.2 Hz, 1 H), 8.85 (dd, *J* = 7.3, 1.0 Hz, 1 H), 8.51 (d, *J* = 8.3 Hz, 1 H), 8.00 (dd, *J* = 8.1, 7.4 Hz, 1 H), 7.50 (t, *J* = 7.8 Hz, 1 H), 7.35 (d, *J* = 7.8 Hz, 2 H), 2.70 (sept, *J* = 6.8 Hz, 2 H), 1.16 (dd, *J* = 6.9, 1.8, Hz, 12 H). ^{13}C NMR (101 MHz, $CDCl_3$) δ 163.29, 162.67, 146.62, 145.68, 136.00, 135.12, 131.42, 130.95, 130.25, 130.02, 129.34, 124.92, 124.89, 124.35, 123.34, 29.39, 24.14, 24.11. IR (ATR) ν (cm^{-1}): 3084, 2967, 2930, 2870, 1717, 1674, 1593, 1541, 1506, 1416, 1366, 1344, 1329, 1240, 1206, 1180, 1144, 1115, 1074, 1057, 1040, 945, 924, 910, 876, 853. ESI-HRMS: $[M+Na]^+$ calc. for $[C_{24}H_{22}N_2O_4Na]^+$: 425.1472; found 425.1470.

2.2 Synthesis of 4

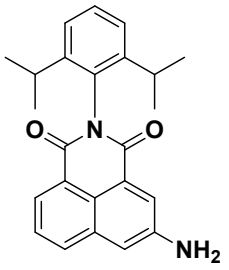

In a round bottom flask, **3** (2.0 g, 4.97 mmol) was added and dissolved in a mixture of EtOAc/EtOH (200 and 80 mL respectively). The reaction was then degassed by argon bubbling and sonication for 5 min. and $SnCl_2{\cdot}2H_2O$ (4.7 g, 24.8 mmol) was then added, followed by further 5 min. degassing. The reaction was then heated at 60°C for 18 h under Ar atmosphere. The resulting bright yellow solution was then concentred under reduced pressure and a sat. solution of K_2CO_3 added. The resulting suspension was extracted with EtOAc (3 × 100 mL), and the resulting organic layer washed with H_2O (2 × 100 mL) and brine (100 mL). The EtOAc solution was the dried over Na_2SO_4, filtered and evaporated under reduced pressure to afford a yellow solid which was further purified using a silica gel plug (CH_2Cl_2) to give **4** as a bright yellow solid (1.47 g, 79%).

M.P.:>300°C. ^{1}H NMR (400 MHz, $CDCl_3$) δ 8.38 (dd, *J* = 7.2, 1.1 Hz, 1 H), 8.11 (d, *J* = 2.4 Hz, 1 H), 8.01 (d, *J* = 8.4 Hz, 1 H), 7.66 (dd, *J* = 8.2, 7.3 Hz, 1 H), 7.46 (t, *J* = 7.7 Hz, 1 H), 7.38 (d, *J* = 2.4 Hz, 1 H), 7.32 (d, *J* = 7.7 Hz, 2 H), 4.26 (bs, 2H), 2.74 (sept, *J* = 6.9 Hz, 2 H), 1.15 (d, *J* = 6.9 Hz, 12 H). ^{13}C NMR (101 MHz, CD_2Cl_2) δ 165.10, 164.92, 146.66, 146.24, 134.31, 132.62, 132.07, 129.81, 128.15, 127.82, 124.52, 124.12, 123.63, 123.04, 122.87, 114.67, 29.58, 24.24, 24.22. IR (ATR) ν (cm^{-1}): 3462, 3370, 2967, 2932, 2868, 1695, 1651, 1632, 1616, 1597, 1578, 1516, 1470, 1445, 1383, 1371, 1362, 1341, 1304, 1254, 1231, 1215, 1179, 1169, 1140, 1098, 1057, 989, 955, 937, 924, 874, 858, 833, 818, 800. ESI-HRMS: $[M+Na]^+$ calc. for $[C_{24}H_{24}N_2O_2Na]^+$: 395.1730; found 395.1776.

2.3 Synthesis of 5

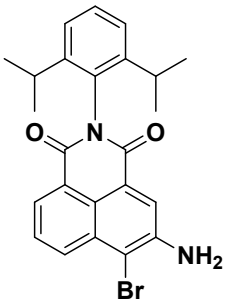

In a round bottom flask, **4** (1.0 g, 2.68 mmol) was added and dispersed in dioxane (30 mL). The resulting yellow suspension was heated to 80°C until complete dissolution of XX. Br_2 (145 µL, 2.83 mmol) was then added dropwise at the same temperature resulting in the formation of a faint yellow precipitate. After 1 h the reaction was filtered and washed extensively with PE. The faint yellow solid was then dispersed in CH_2Cl_2 (100 mL) and washed with a sat. aq. solution of $NaHCO_3$ followed by a sodium thiosulfate one (1 g in 100 mL), H_2O (50 mL) and brine (50 mL). The organic layers were then dried over Na_2SO_4, filtered and evaporated to give **5** as a dark yellow powder (1.04 g, 86%).

M.P.:297 °C. ^{1}H NMR (400 MHz, $CDCl_3$) δ 8.44 (dd, *J* = 2.9, 0.9 Hz, 1 H), 8.42 (dd, *J* = 4.3, 1.0 Hz, 1 H), 8.19 (s, 1 H), 7.78 (dd, *J* = 8.5, 7.3 Hz, 1 H), 7.47 (t, *J* = 7.8 Hz, 1 H), 7.32 (d, *J* = 7.8 Hz, 2 H), 4.71 (bs, 2 H), 2.71 (sept. *J* = 6.9 Hz, 2 H), 1.15 (dd, *J* = 6.9, 1.4 Hz, 12 H). ^{13}C NMR (101 MHz, $CDCl_3$) δ 164.16, 163.96, 145.78, 143.50, 132.33, 131.47, 130.82, 129.71, 128.59, 128.37, 124.18, 123.65, 122.93, 122.75, 122.06, 110.58, 29.28, 24.11, 24.09. IR (ATR) ν (cm^{-1}): 3464, 3348, 3071, 2961, 2926, 2868, 1703, 1668, 1614, 1597, 1562, 1506, 1466, 1447, 1423, 1383, 1337, 1292, 1256, 1233, 1209, 1194, 1144, 1098, 1057, 1009, 980, 972, 951, 939, 920, 899, 883, 837, 800. ESI-HRMS: $[M+H]^+$ calc. for $[C_{24}H_{24}BrN_2O_2]^+$: 451.1016; found 451.1016.

2.4 Synthesis of 1

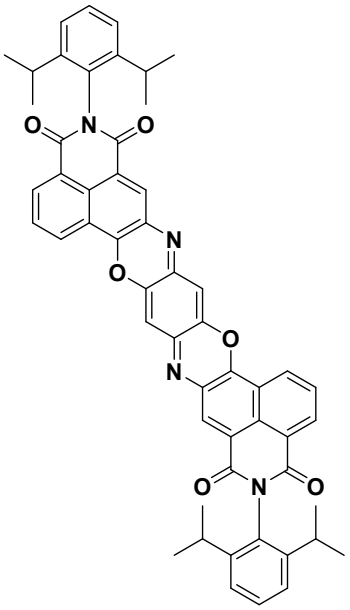

In a Microwave vial **5** (500 mg, 1.11 mmol) was added along with 2,5-dihydroxybenzoquinone **6** (78 mg, 0.55 mmol) and suspended in 1.0 mL of heptanoic acid. The reaction was then heated under MW irradiation at 200 °C for 1h. After cooling down, the black tar was suspended in Et_2O (10 mL), sonicated and centrifuged (6000 rpm, 10 min.). The precipitate was again suspended in Et_2O (8 mL) and Et_3N (2 mL), sonicated and again centrifuged. Finally, the solid was suspended, sonicated and centrifuged 3 times from methanol. The dark red solid was then purified via a neutral alumina plug (CH_2Cl_2 100% to CH_2Cl_2/EtOAc 95/5) to give **1** as a bright red amorphous solid (231 mg, 50%). Further purification can be achieved by repeated cycles of precipitation/centrifugation from MeOH/CH_2Cl_2, MeOH and Et_2O.

^{1}H NMR (500 MHz, CD_2Cl_2) δ 8.71 (d, *J* = 8.4 Hz, 2H), 8.68-8.65 (m, 4H), 7.91 (dd, *J* = 8.4, 7.3 Hz, 2H), 7.51 (t, *J* = 7.8 Hz, 2H), 7.35 (d, *J* = 7.8 Hz, 4H), 6.89 (s, 2 H), 2.77-2.71 (m, 4H), 1.14 (d, *J* = 6.8, 12H), 1.13 (d, *J* = 6.8 Hz, 12H). ^{13}C NMR (126 MHz, CD_2Cl_2) δ 164.48, 163.70, 153.51, 148.74, 146.61, 144.94, 133.24, 132.98, 132.52, 131.70, 130.00, 129.68, 128.47, 128.36, 124.61, 123.59, 122.11, 120.24, 108.11, 29.67, 24.26. IR (ATR) ν (cm^{-1}): 3073, 3028, 2970, 2924, 2868, 1709, 1672, 1597, 1568, 1427, 1364, 1341, 1256, 1236, 1194, 1171, 918, 905, 893, 839, 802, 789, 781, 747, 731. ESI-HRMS: $[M+H]^+$ calc. for $[C_{54}H_{45}N_4O_6]^+$: 845.3334; found 845.3320.

^{1}H NMR (500 MHz, TFA-*d*1) δ 8.99-8.97 (m, 6H), 8.14 (t, *J* = 7.9 Hz, 2H), 7.70 (s, 2H), 7.53 (t, *J* = 7.9 Hz, 2H), 7.39 (d, *J* = 7.9 Hz, 4H), 2.63 (p, *J* = 6.7 Hz, 4H), 1.13 (dd, *J* = 7.1, 3.3 Hz, 24H). ^{13}C (126 MHz, TFA-*d*1) δ 166.33, 165.20, 150.69, 149.00, 146.39, 145.84, 136.69, 131.38, 130.21, 130.16, 130.02, 128.52, 128.42, 127.97, 125.33, 122.07, 121.68, 120.98, 107.24, 29.46, 22.69, 22.67.

^{1}H NMR (400 MHz, TFA-*d*1/D_2SO_4) δ 9.22 (d, *J* = 8.7 Hz, 2H), 9.18 – 9.16 (m, 4H), 8.31 (t, *J* = 8.0 Hz, 2H), 8.24 (s, 2H), 7.64 (t, *J* = 7.9 Hz, 2H), 7.48 (d, *J* = 7.7 Hz, 4H), 2.68 (p, *J* = 6.9 Hz, 4H), 1.20 (dd, *J* = 6.8 Hz, 1.8 Hz, 24H).

2.5 Synthesis of 7

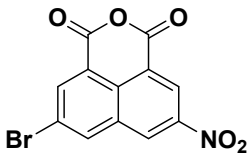

In a round bottom flask, 2-nitronaphthalene-1,3-monoanydride **2** (1.0 g, 4.1 mmol) was added together with AgOAc (686 mg, 4.1 mmol) and suspended in H_2SO_4 (20 mL). Br_2 (263 µL, 5.1 mmol) was then added, and the resulting suspension heated at 100°C for 18 h. The resulting dark suspension was then allowed to cool to r.t., dropped in H_2O and filtered followed by washing with MeOH. The resulting beige powder was recrystallized from toluene to give 743 mg of **7** as a beige solid (743 mg, 56%).

^{1}H NMR (400 MHz, $CDCl_3$) δ δ 9.33 (d, *J* = 2.1 Hz, 1H), 9.15 (d, *J* = 2.1 Hz, 1H), 8.87 (d, *J* = 1.9 Hz, 1H), 8.70 (d, *J* = 1.8 Hz, 1H). ^{13}C NMR (101 MHz, $CDCl_3$) δ 158.15, 158.09, 147.29, 139.46, 138.65, 132.56, 130.61, 129.26, 126.54, 124.19, 121.32, 120.89. IR (ATR) ν (cm^{-1}): 3088, 1782, 1746, 1586, 1530, 1501, 1422, 1389, 1333, 1269, 1229, 1159, 1134, 1086, 1063, 1020, 955, 939, 920, 893, 874, 802, 758, 737, 714, 691.

2.6 Synthesis of 8

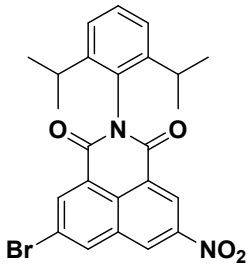

In a round bottom flask, 2-nitro-6-bromonaphthalene-1,3-monoanydride **7** (500 mg, 1.55 mmol) was added and suspended in AcOH (10 mL). 2,6-diisopropyl aniline (307 µL, 1.63 mmol) was then added, and the resulting suspension heated at 110°C for 18 h. The brown solution was then allowed to cool to r.t., dropped in H_2O and filtered followed by washing with small amounts of cold MeOH and Et_2O to give a beige solid (622 mg, 83%) which was directly used in the following step.

^{1}H NMR (400 MHz, $CDCl_3$) δ 9.35 (d, *J* = 2.1 Hz, 1H), 9.12 (d, *J* = 2.1 Hz, 1H), 8.88 (d, *J* = 1.8 Hz, 1H), 8.66 (d, *J* = 1.6 Hz, 1H), 7.51 (t, *J* = 7.8 Hz, 1H), 7.35 (d, *J* = 7.8 Hz, 2H), 2.71-2.61 (m, 2H), 1.15 (d, *J* = 6.8 Hz, 12H).^{13}C NMR (101 MHz, $CDCl_3$) δ 162.24, 162.19, 147.30, 145.63, 137.94, 137.43, 132.64, 130.20, 129.92, 129.36, 128.14, 125.07, 125.02, 124.63, 124.43, 123.90, 29.43, 24.11. IR (ATR) ν (cm^{-1}): 3086, 2967, 2870, 1717, 1676, 1597, 1539, 1506, 1464, 1398, 1339, 1310, 1240, 1204, 1182, 1084, 1057, 984, 910, 870, 839, 806, 801, 756, 737, 729, 710, 601. ESI-LRMS $[M+H]^+$ calc. for $[C_{24}H_{22}{}^{79}BrN_2O_4]^+$: 481.08; found 481.08.

2.7 Synthesis of 9

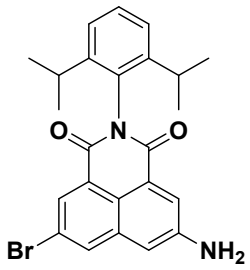

In a round bottom flask **8** (737 mg, 1.53 mmol) was added and dissolved in a mixture of EtOAc/EtOH (40 and 16 mL respectively). The reaction was then degassed by argon bubbling and sonication for 5 min. and $SnCl_2 \cdot 2H_2O$ (1.45 g, 7.65 mmol) was then added, followed by further 5 min. degassing. The reaction was then heated at 60°C for 18 h under Ar atmosphere. The resulting bright yellow solution was then concentred under reduced pressure and a sat. solution of K_2CO_3 added. The resulting suspension was extracted with EtOAc (3 × 100 mL), and the resulting organic layer washed with H_2O (2 × 100 mL) and brine (100 mL). The EtOAc solution was the dried over Na_2SO_4, filtered and evaporated under reduced pressure to afford a yellow solid which was further purified using a silica gel plug (CH_2Cl_2) to give **8** as a bright yellow solid (356 mg, 52%).

^{1}H NMR (400 MHz, $CDCl_3$) δ 8.41 (d, *J* = 1.8 Hz, 1H), 8.14 (d, *J* = 1.8 Hz, 1H), 8.07 (d, *J* = 2.3 Hz, 1H), 7.49 – 7.45 (m, 1H), 7.32 (d, *J* = 7.8 Hz, 2H), 7.25 (d, *J* = 2.3 Hz, 1H), 4.26 (s, 2H), 2.75-2.65 (m, 2H), 1.14 (dd, *J* = 6.8, 1.5 Hz, 12H). ^{13}C NMR (101 MHz, CD_2Cl_2) δ 163.96, 163.53, 146.40, 145.79, 135.22, 133.53, 130.75, 130.56, 129.75, 124.22, 124.09, 122.85, 121.77, 121.70, 112.65, 29.27, 24.11. IR (ATR) ν (cm^{-1}): 3497, 3374, 3219, 3069, 2963, 2905, 2868, 1705, 1667, 1626, 1614, 1512, 1412, 1385, 1329, 1290, 1233, 1217, 1057, 997, 959, 939, 876, 837, 808, 801, 779, 745, 718. ESI-LRMS $[M+H]^+$ calc. for $[C_{24}H_{24}{}^{79}BrN_2O_2]^+$: 451.10; found 451.17.

2.8 Synthesis of 10

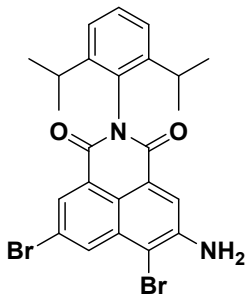

In a round bottom flask, **9** (300 mg, 0.67 mmol) was added and dispersed in dioxane (15 mL). Br_2 (36 µL, 0.7 mmol) was then added dropwise resulting in the formation of a faint yellow precipitate. After 1 h the reaction was filtered and washed extensively with PE. The faint yellow solid was then dispersed in CH_2Cl_2 (100 mL) and washed with a sat. aq. solution of $NaHCO_3$ followed by a sodium thiosulfate one (1 g in 100 mL), H_2O (50 mL) and brine (50 mL). The organic layers were then dried over Na_2SO_4, filtered and evaporated reprecipitation from MeOH afforded **10** as a yellow powder (303 mg, 86%).

^{1}H NMR (400 MHz, $CDCl_3$) δ 8.57 (d, *J* = 1.8 Hz, 1H), 8.48 (d, *J* = 1.8 Hz, 1H), 8.14 (s, 1H), 7.50 – 7.46 (m, 1H), 7.32 (d, *J* = 7.8 Hz, 2H), 4.78 (s, 2H), 2.73-2.62 (m, 2H), 1.14 (dd, *J* = 6.8, 2.6 Hz, 12H). ^{13}C NMR (101 MHz, $CDCl_3$) δ 163.57, 163.13, 145.75, 144.36, 133.72, 133.25, 130.95, 130.50, 129.88, 124.36, 124.27, 123.36, 122.77, 122.30, 122.07, 108.56, 29.32, 24.09. IR (ATR) ν (cm^{-1}): 3466, 3350, 3206, 2961, 2926, 2868, 1707, 1672, 1620, 1589, 1557, 1505, 1443, 1416, 1375, 1354, 1317, 1273, 1225, 1192, 1152, 1057, 990, 939, 899, 870, 839, 797, 777, 747, 735, 718. ESI-LRMS $[M+H]^+$ calc. for $[C_{24}H_{23}{}^{79}Br_2N_2O_2]^+$: 531.01; found 531.08.

2.9 Synthesis of 1Br

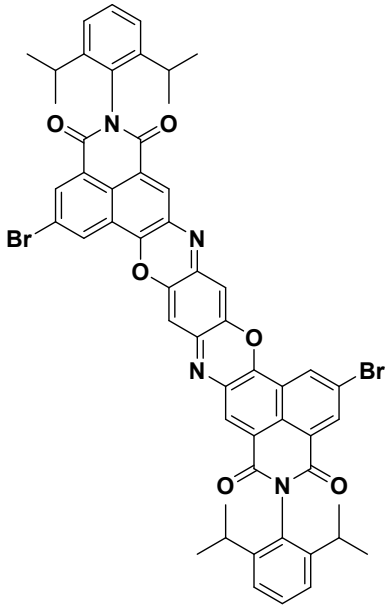

In a Microwave vial **10** (100 mg, 0.19 mmol) was added along with 2,6-dihydroxybenzoquinone **6** (13 mg, 0.09 mmol) and suspended in 100 µL of heptanoic acid. The reaction was then heated under MW irradiation at 200 °C for 30 min. After cooling down, the black tar was diluted in MeOH/Et_3N and evaporated. The dark red solid was then purified via a SCC plug (CH_2Cl_2 100% to CH_2Cl_2/EtOAc 90/10) followed by a preparative TLC in CH_2Cl_2/EtOAc 90/10. As a result, only 8 mg of still impure **1Br** were obtained. Crystals of good enough quality for scXRD were obtained by slow diffusion of hexane in $CHCl_3$.

3 NMR and HRMS spectra

3.1 Characterization of 3

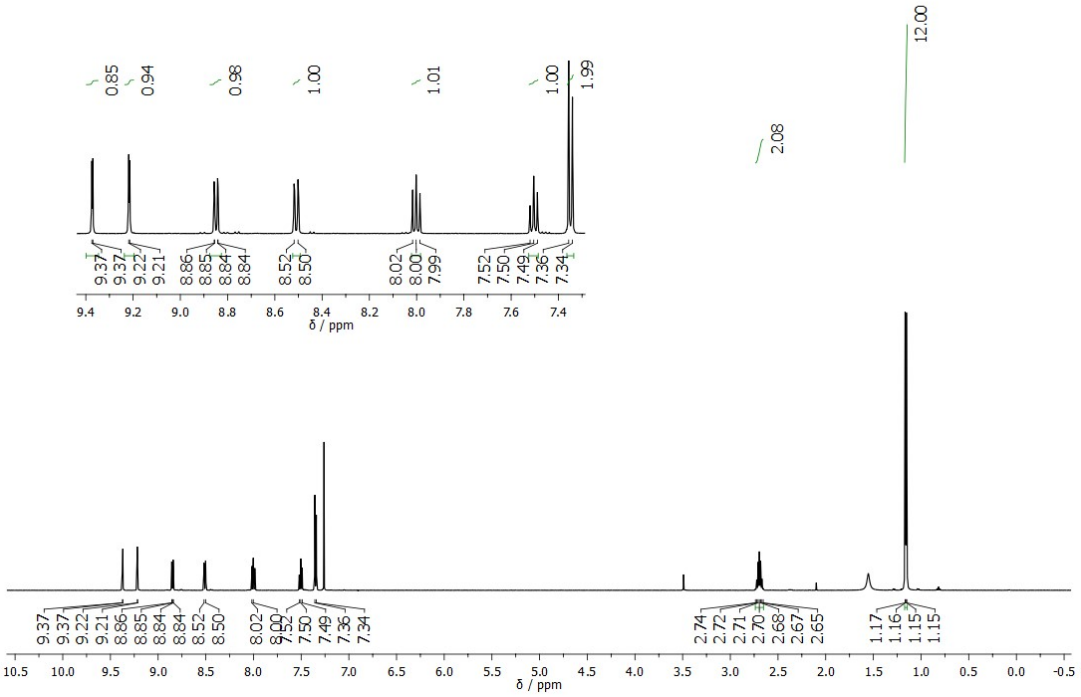

Figure S1. ^{1}H NMR 400 MHz of **3** in $CDCl_3$

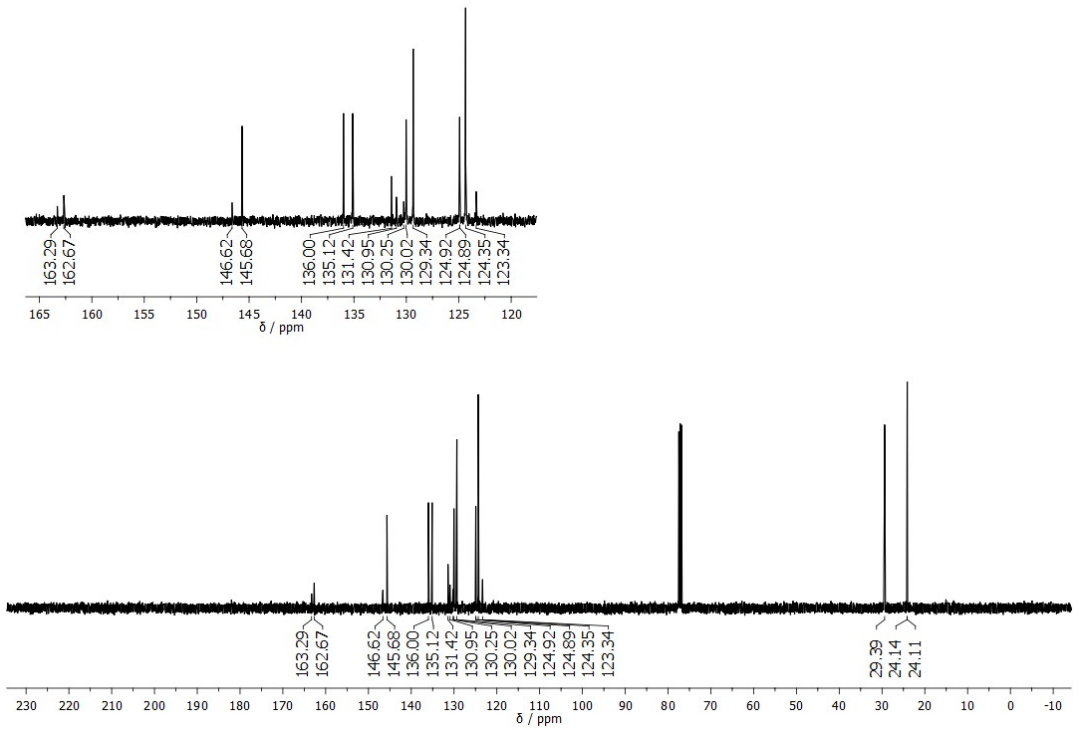

Figure S2. ^{13}C NMR 101 MHz of **3** in $CDCl_3$.

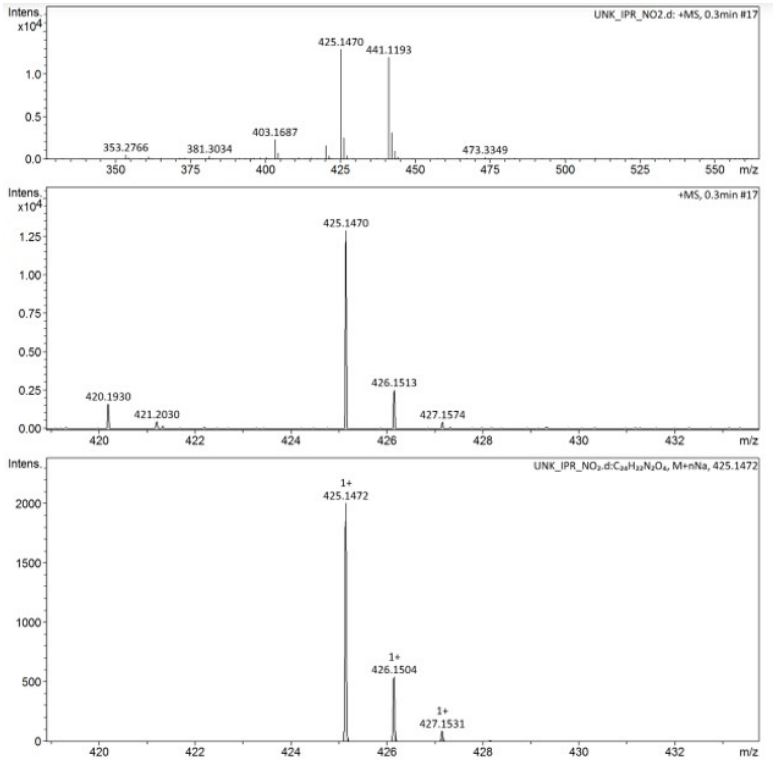

Figure S3. ESI-HRMS of **3**, top) experimental spectra, middle) zoom and bottom) simulated spectra.

3.2 Characterization of 4

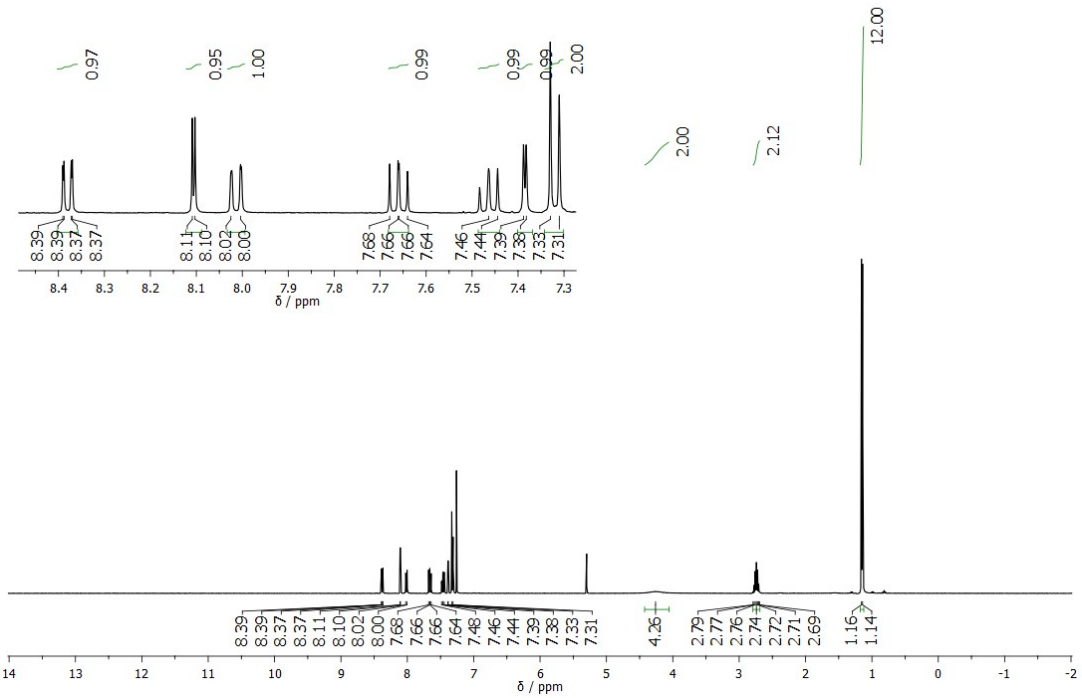

Figure S4. ^{1}H NMR 400 MHz of **4** in $CDCl_3$ (signal at 5.30 is due to residual CH_2Cl_2 traces).

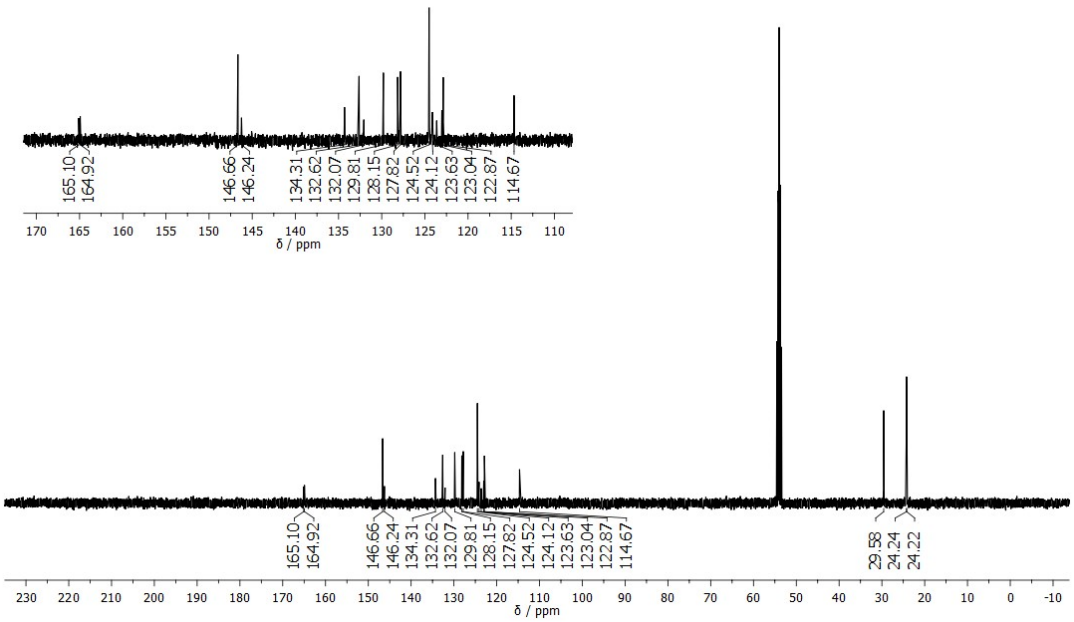

Figure S5. ^{13}C NMR 101 MHz of **4** in $CDCl_3$.

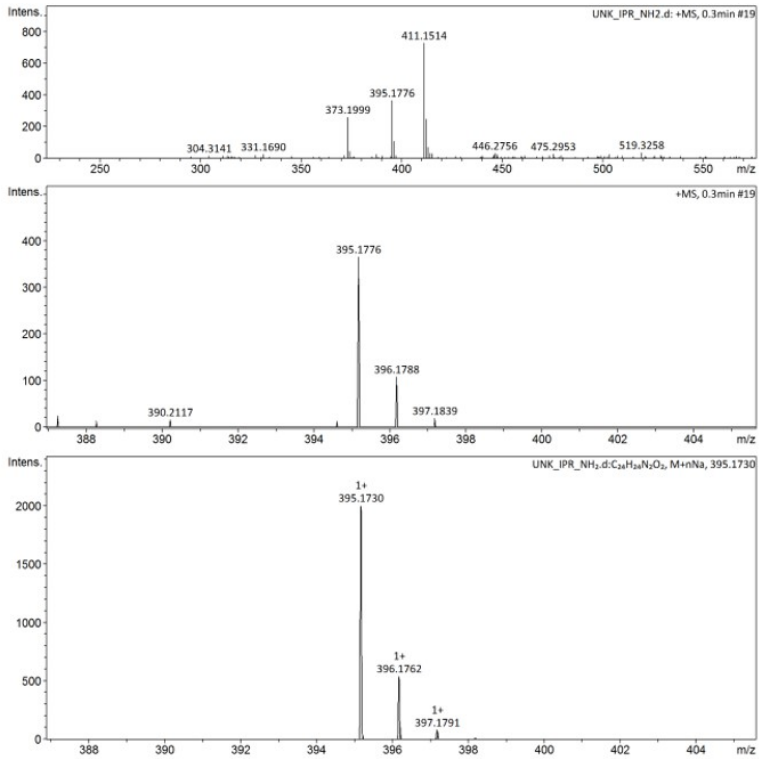

Figure S6. ESI-HRMS of **4**, top) experimental spectra, middle) zoom and bottom) simulated spectra.

3.3 Characterization of 5

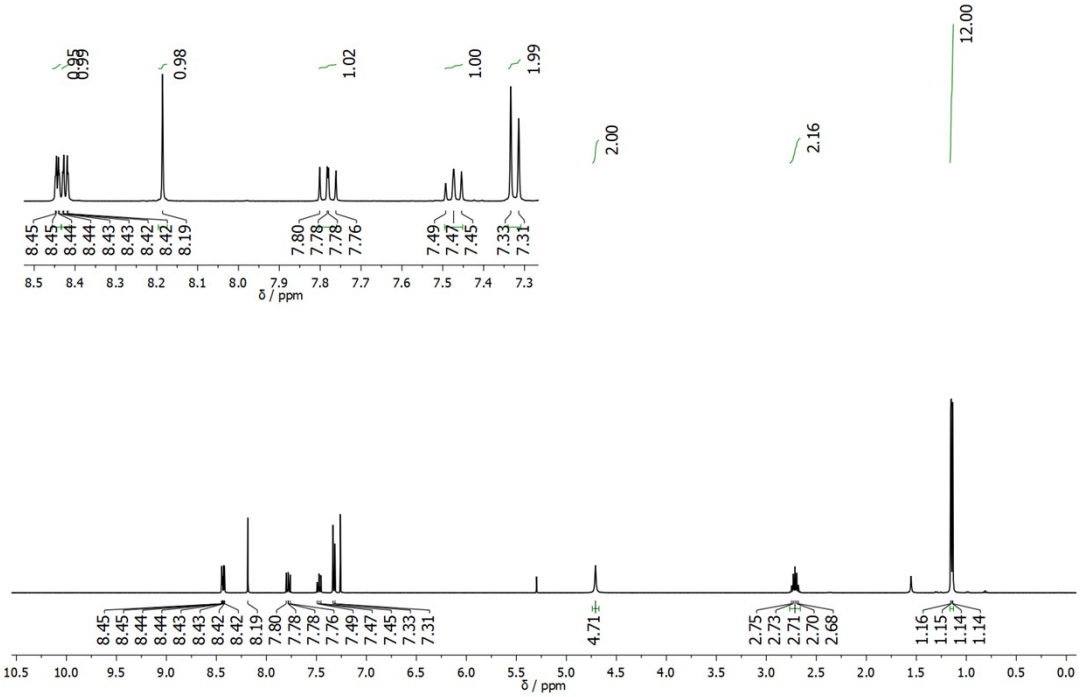

Figure S7. ^{1}H NMR 400 MHz of **5** in $CDCl_3$ (signal at 5.30 is due to residual CH_2Cl_2 traces).

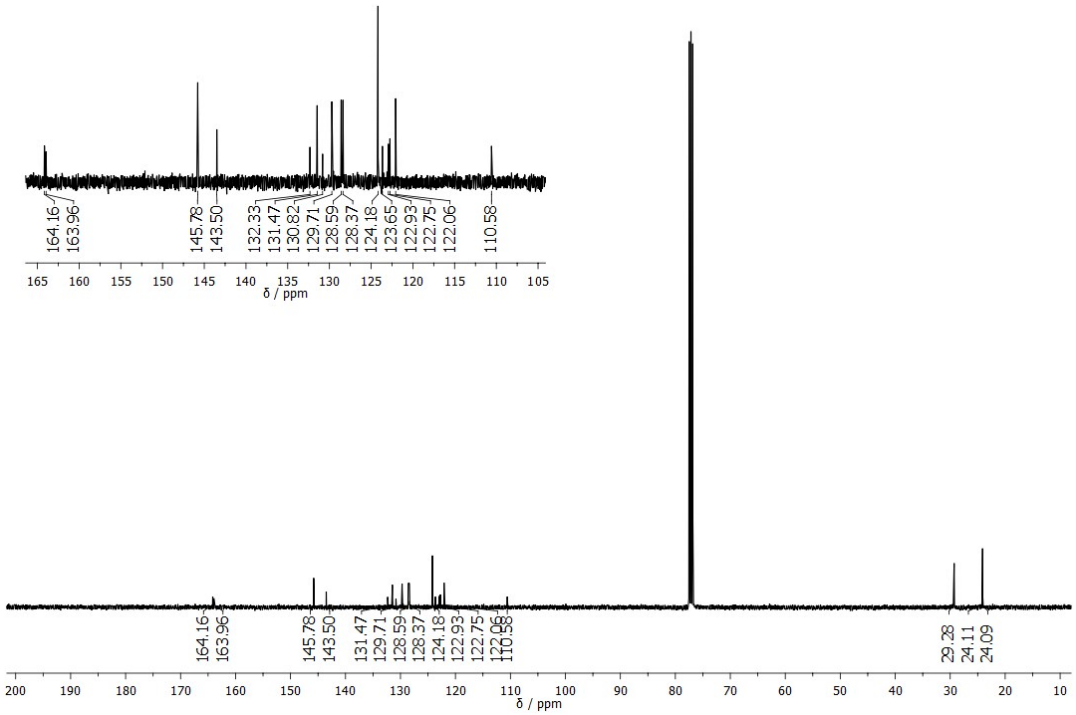

Figure S8. ^{13}C NMR 101 MHz of **5** in $CDCl_3$.

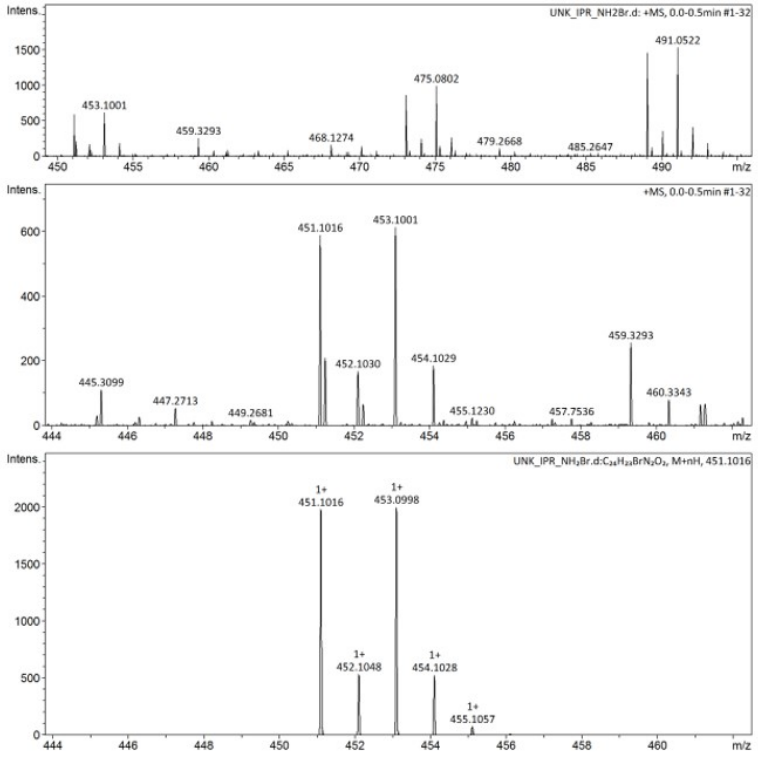

Figure S9. ESI-HRMS of **5**, top) experimental spectra, middle) zoom and bottom) simulated spectra.

3.4 Characterization of 1

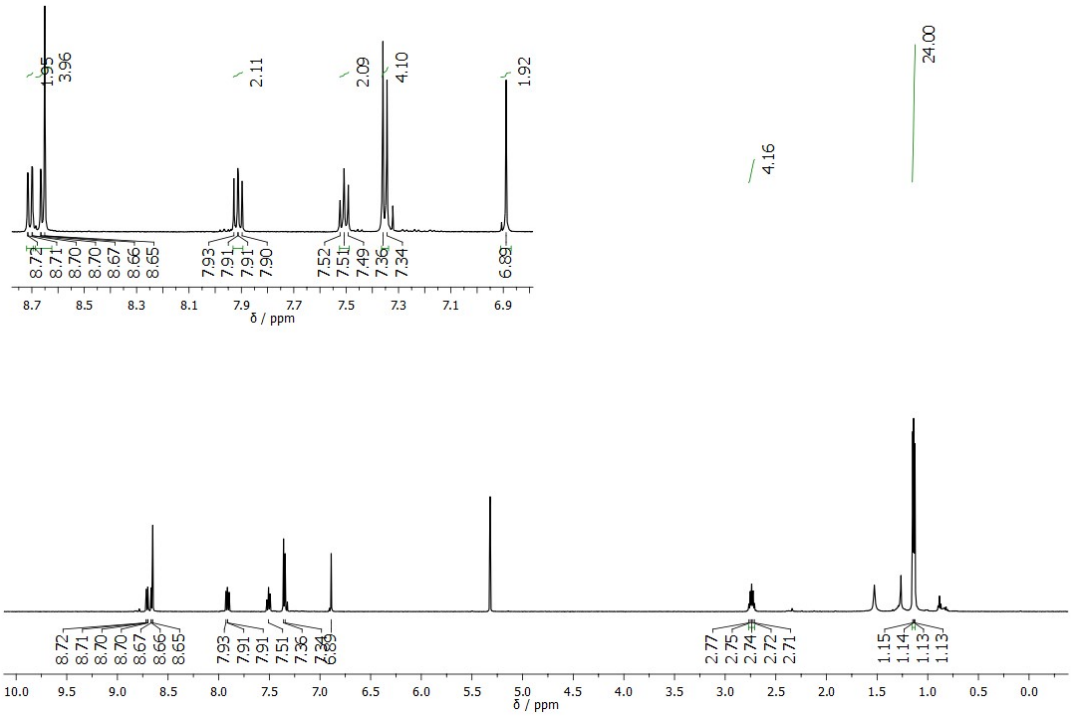

Figure S10. ^{1}H NMR 500 MHz of **1** in CD_2Cl_2.

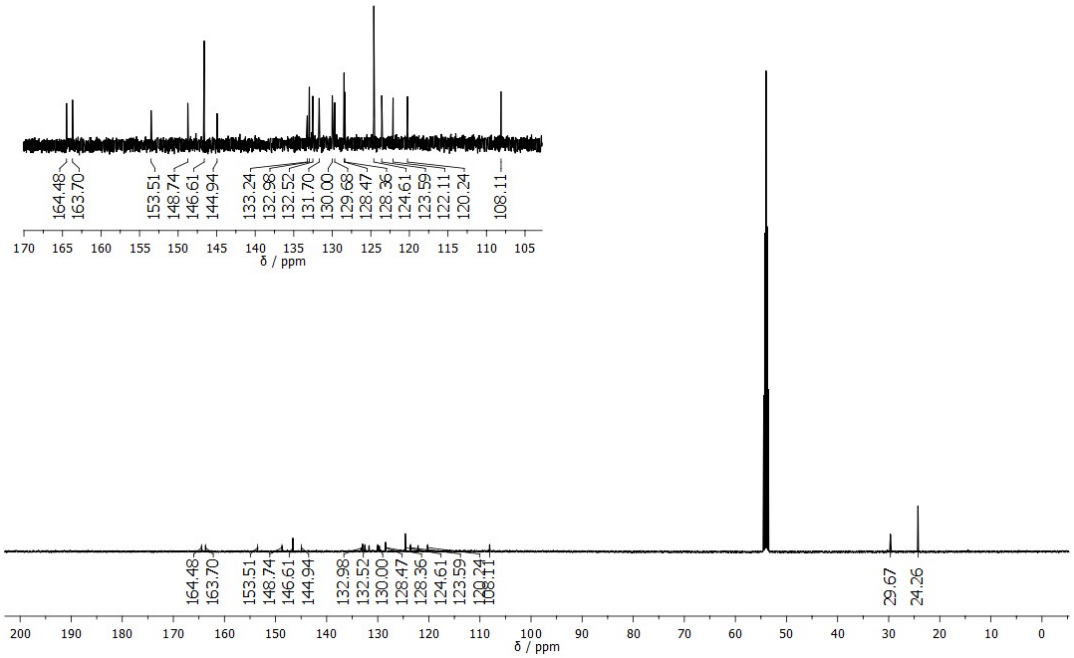

Figure S11. ^{13}C NMR 126 MHz of **1** in CD_2Cl_2.

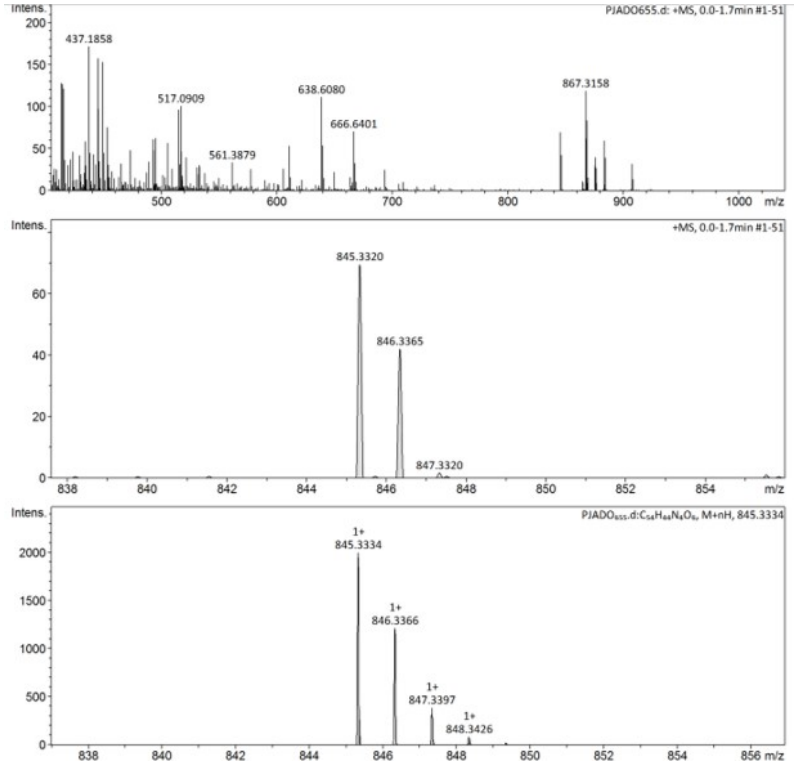

Figure S12. ESI-HRMS of **1**.

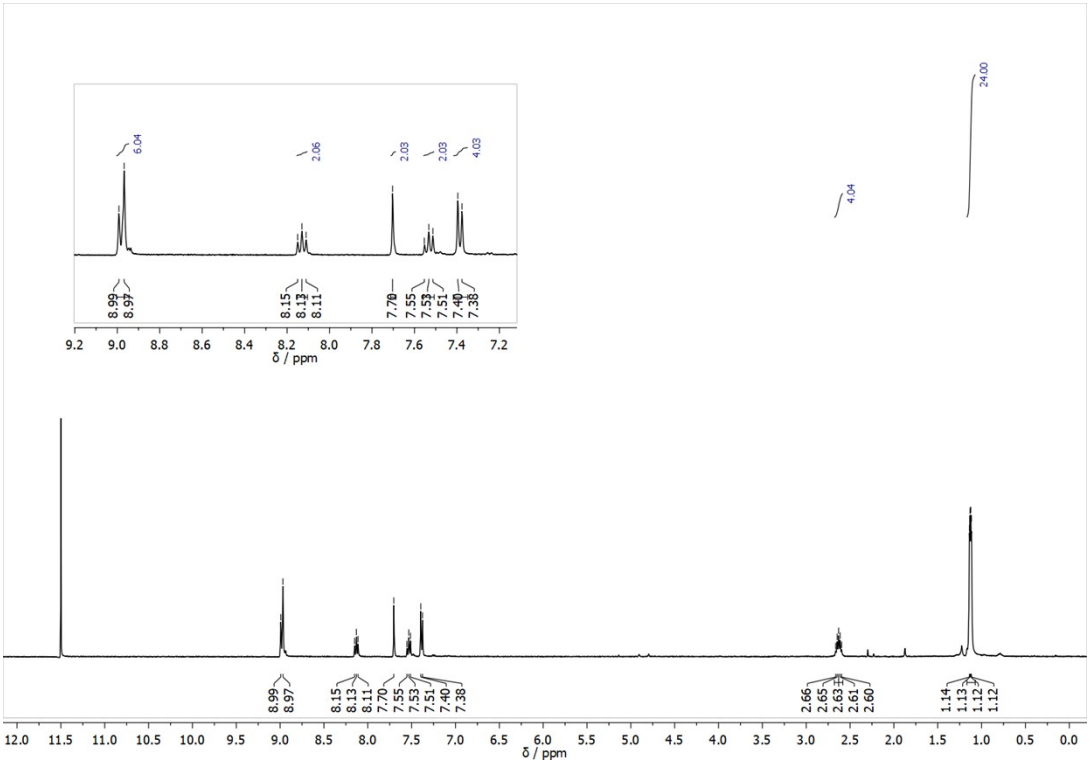

Figure S13. ^{1}H NMR 500 MHz of $\mathbf{1^{H+}}$ in TFA-*d*1.

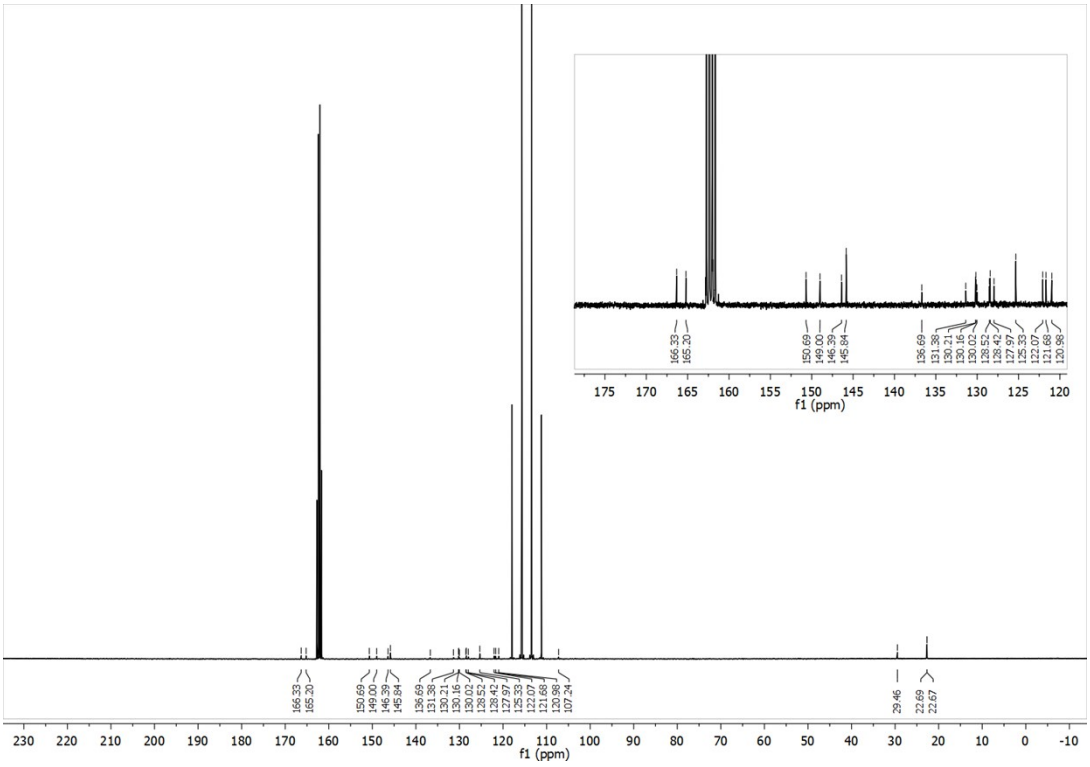

Figure S14. ^{13}C NMR 126 MHz of $\mathbf{1^{H+}}$ in TFA-*d*1.

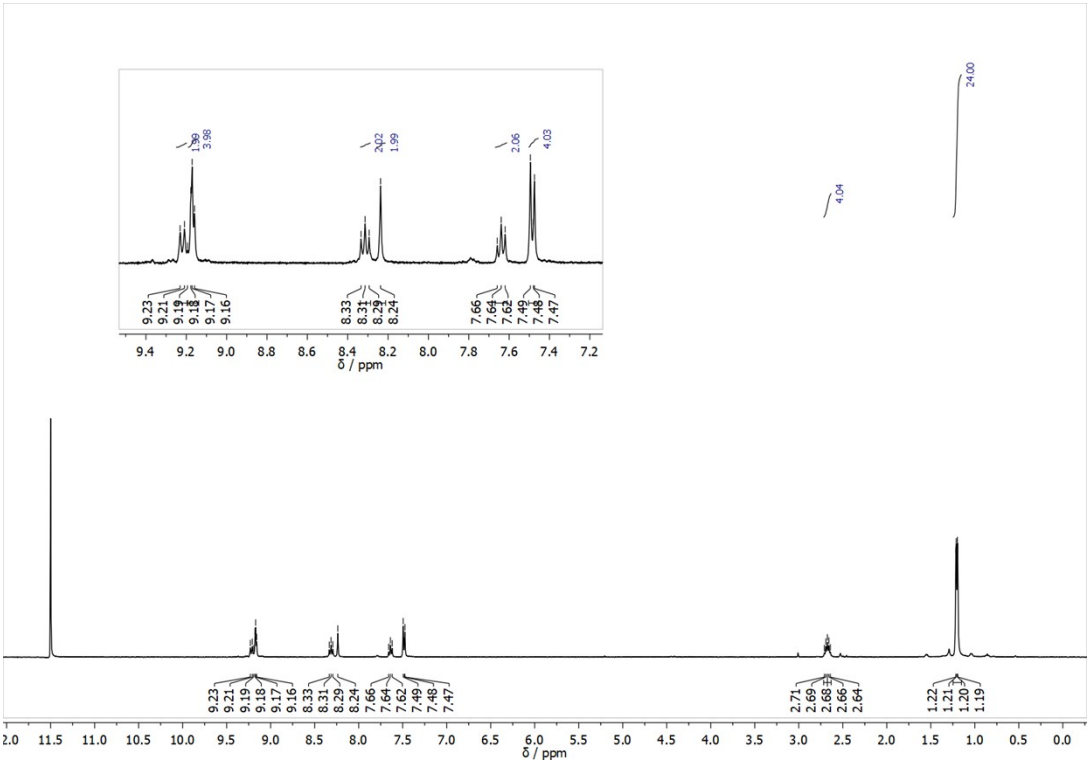

Figure S15. ^{1}H NMR 400 MHz of $\mathbf{1}^{\mathbf{H2+}}$ in TFA-*d*1/D_2SO_4.

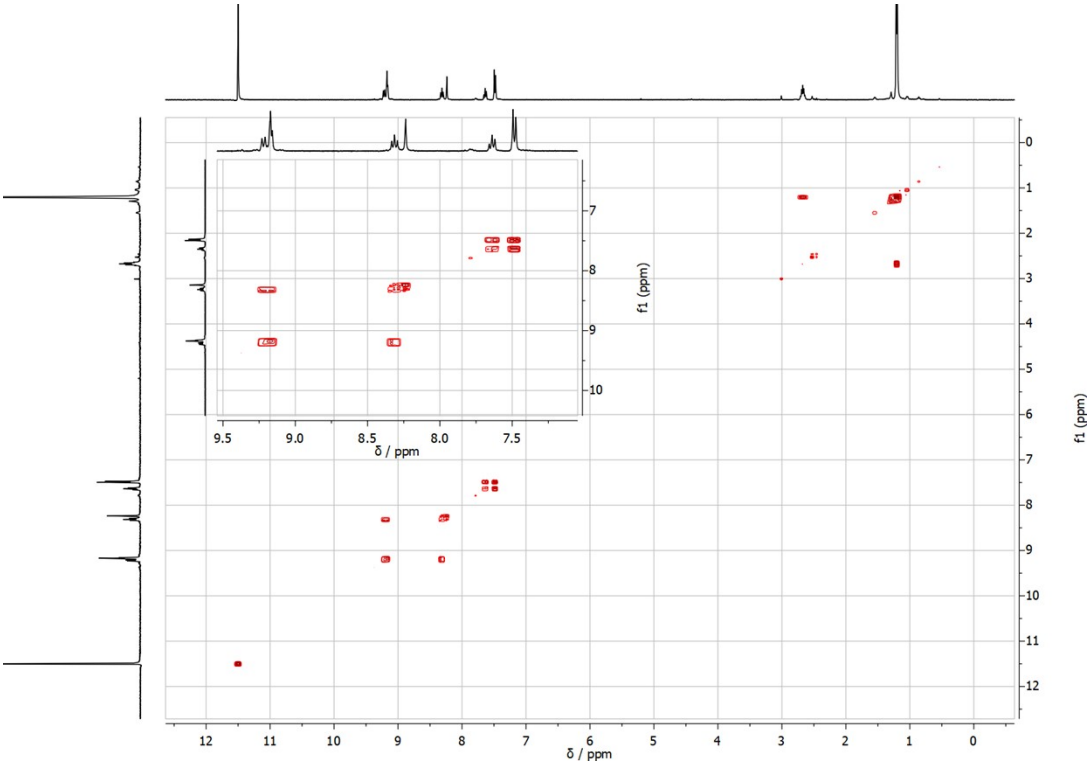

Figure S16. ^{1}H-^{1}H COSY NMR 400 MHz of $\mathbf{1}^{\mathbf{H2+}}$ in TFA-*d*1/D_2SO_4.

3.5 Characterization of 7

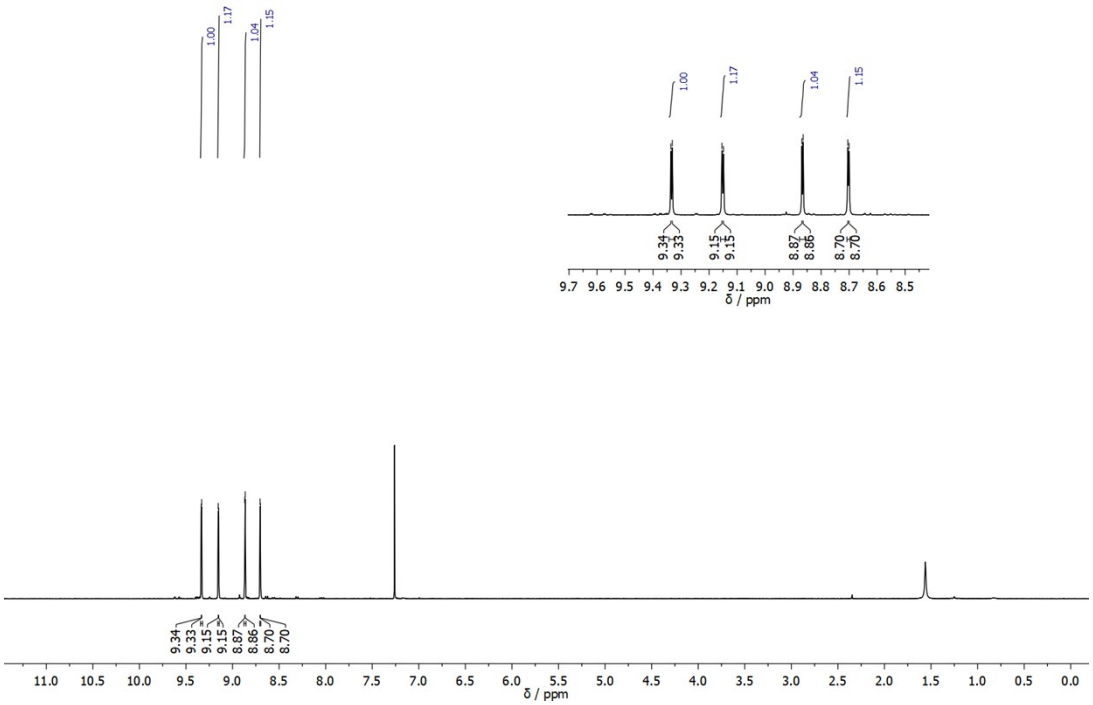

Figure S17. 400 MHz ^{1}H NMR of **7** in $CDCl_3$.

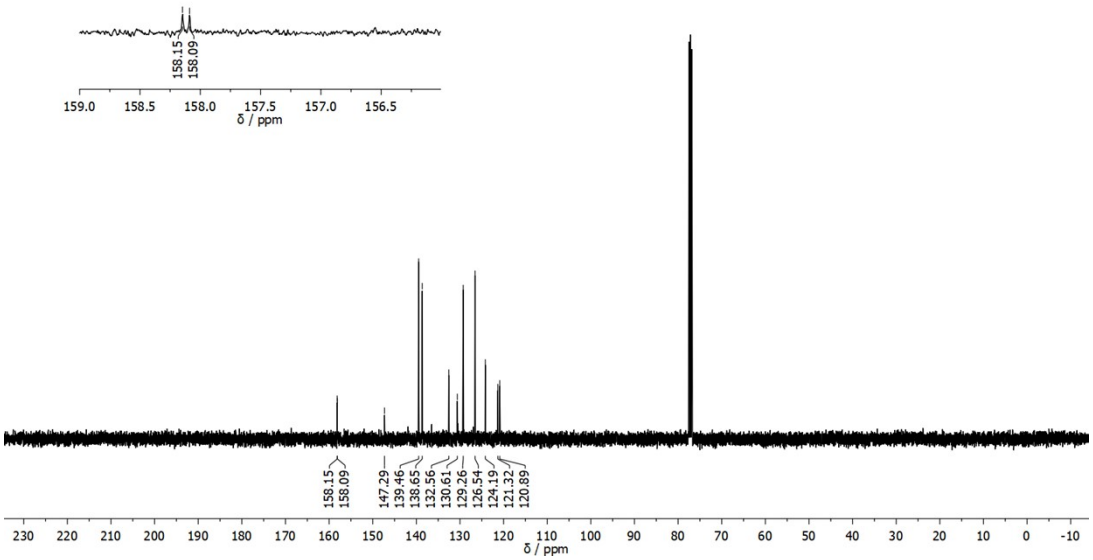

Figure S18. 101 MHz ^{13}C NMR of **7** in $CDCl_3$.

3.6 Characterization of 8

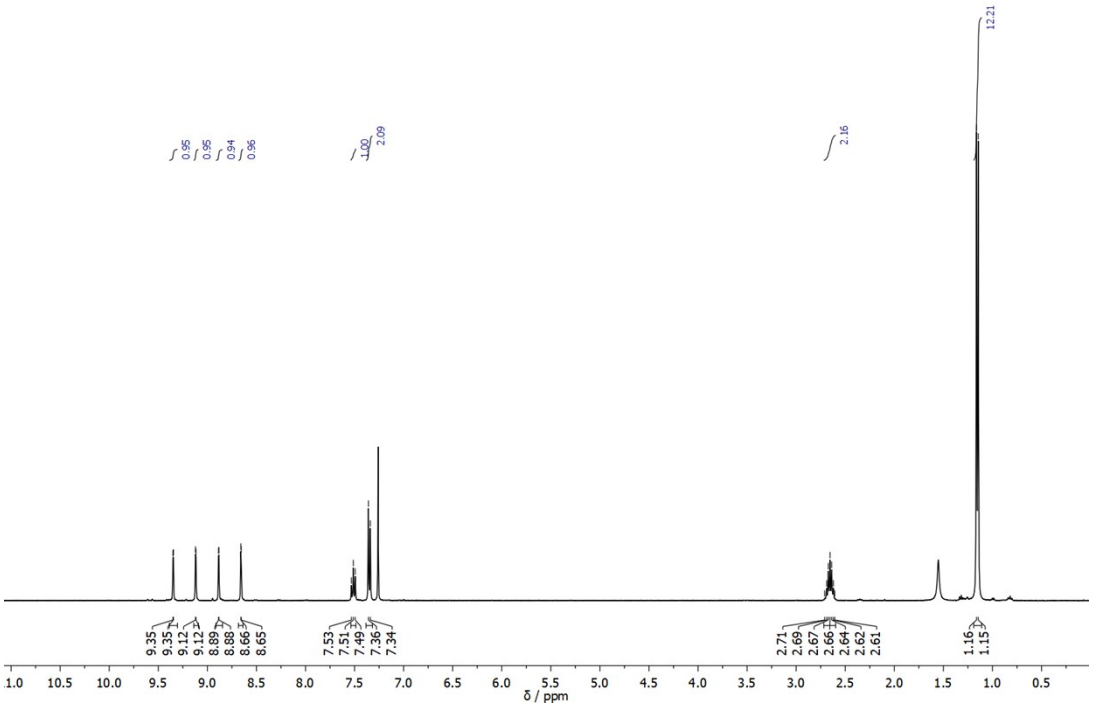

Figure S19. 400 MHz ^{1}H NMR of **8** in $CDCl_3$.

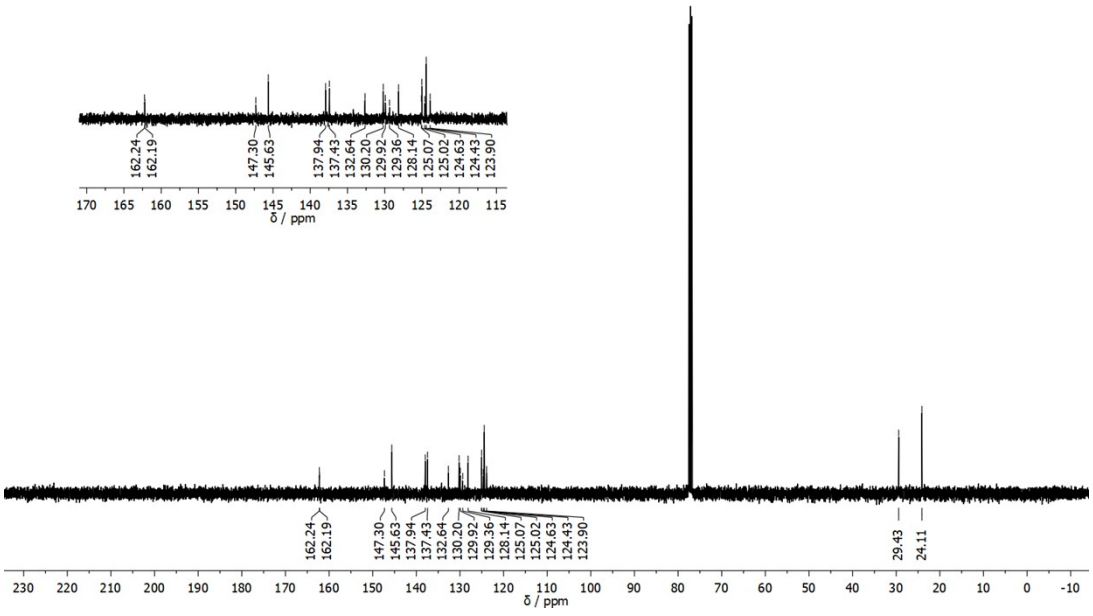

Figure S20. 101 MHz ^{13}C NMR of **8** in $CDCl_3$.

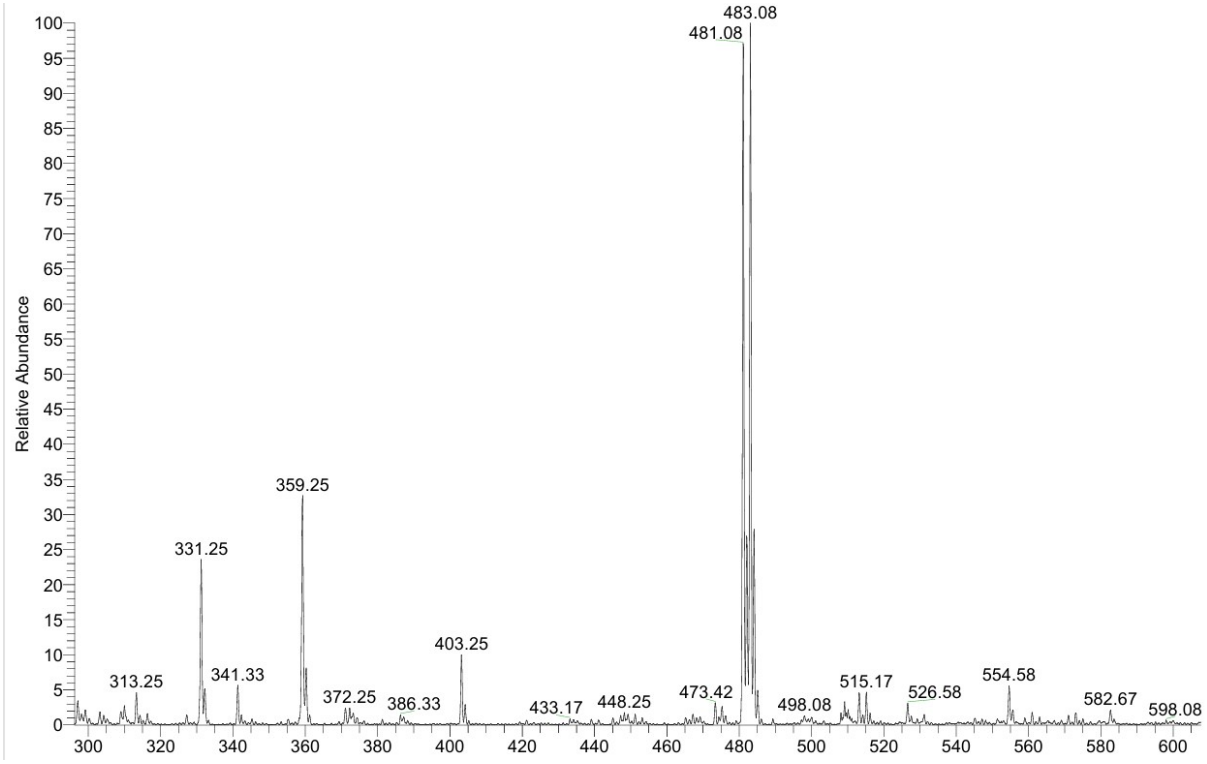

Figure S21. ESI-LRMS of **8**.

3.7 Characterization of 9

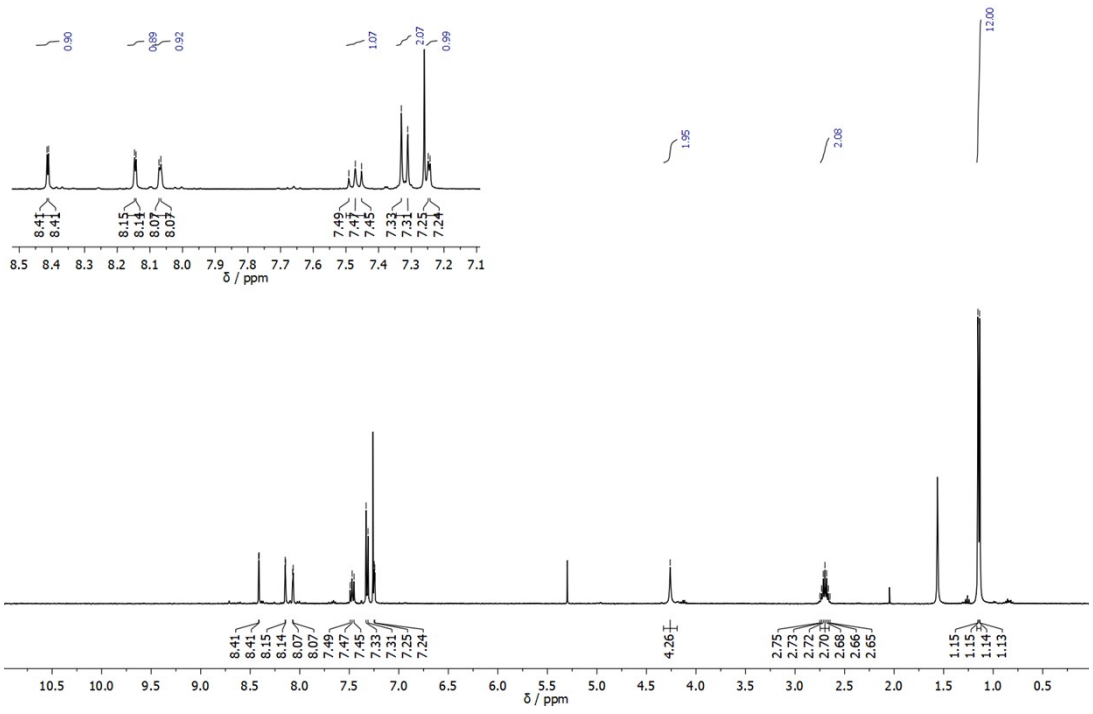

Figure S22. 400 MHz ^{1}H NMR of **9** in $CDCl_3$.

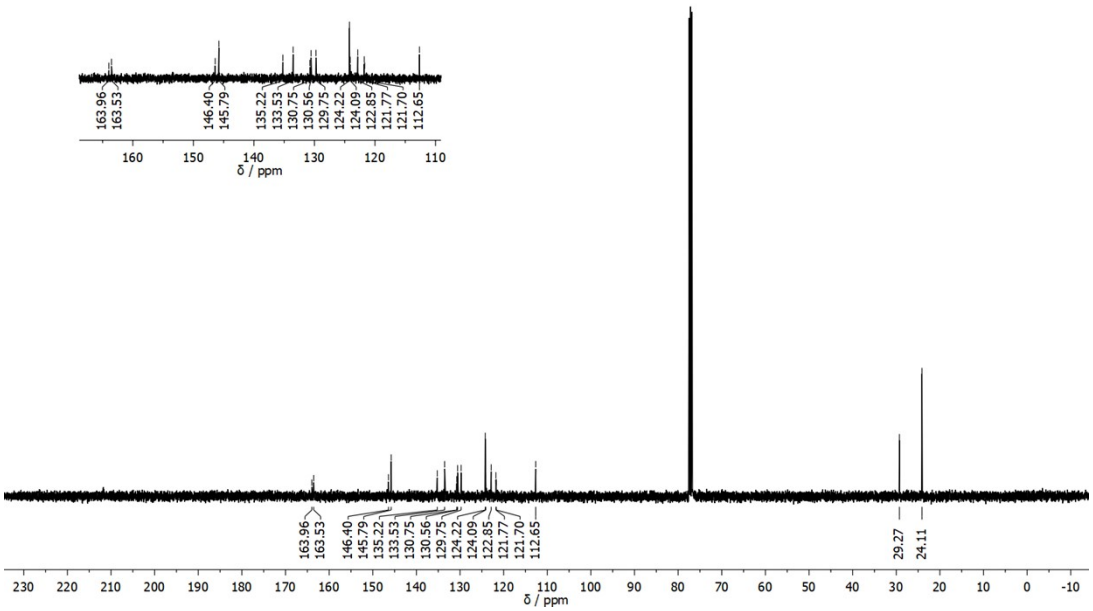

Figure S23. 101 MHz ^{13}C NMR of **9** in $CDCl_3$.

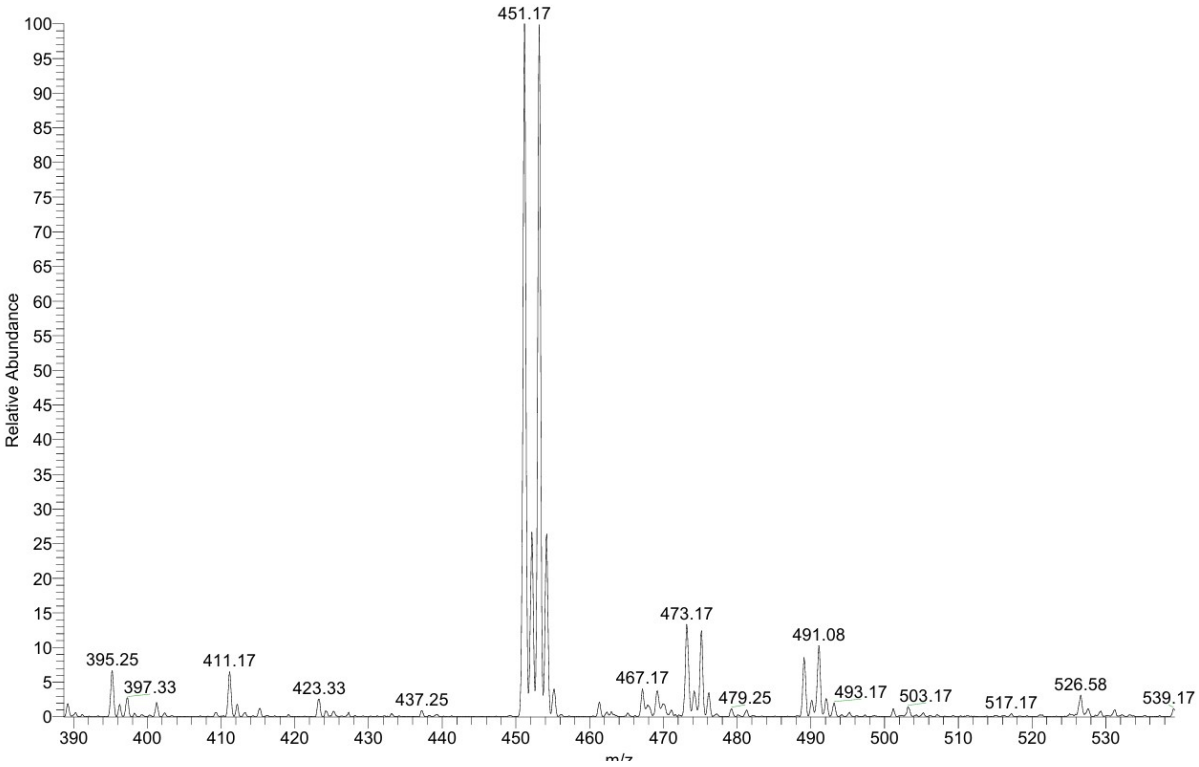

Figure S24. ESI-LRMS of **9**.

3.8 Characterization of 10

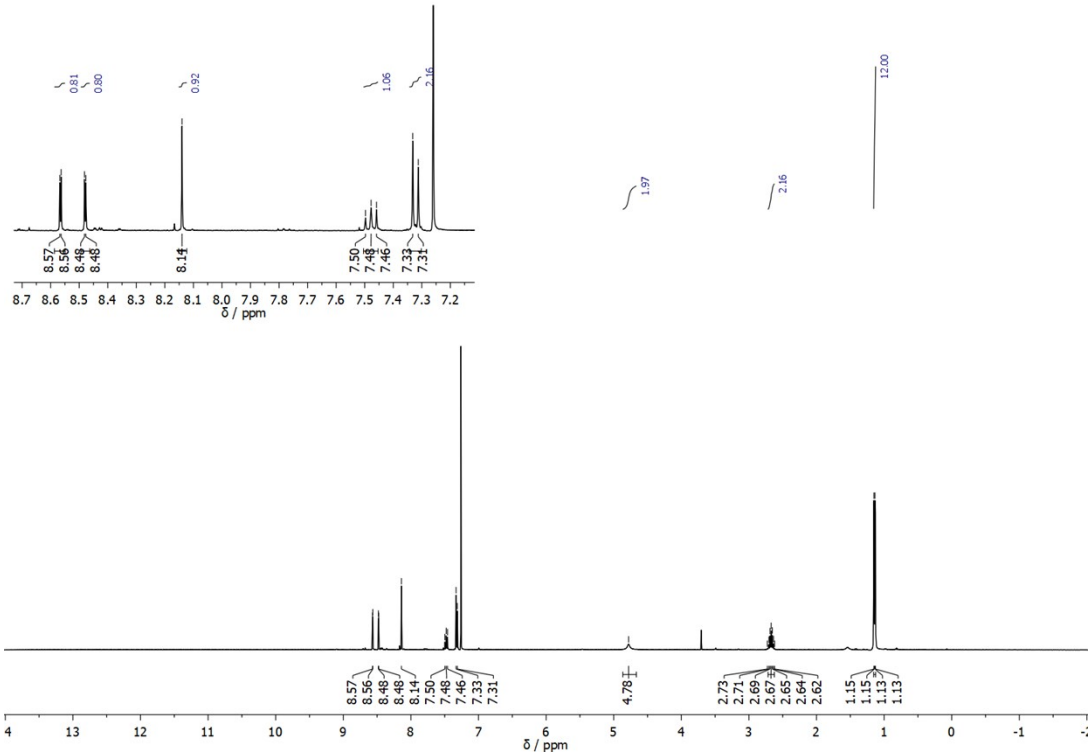

Figure S25. 400 MHz ^{1}H NMR of **10** in $CDCl_3$.

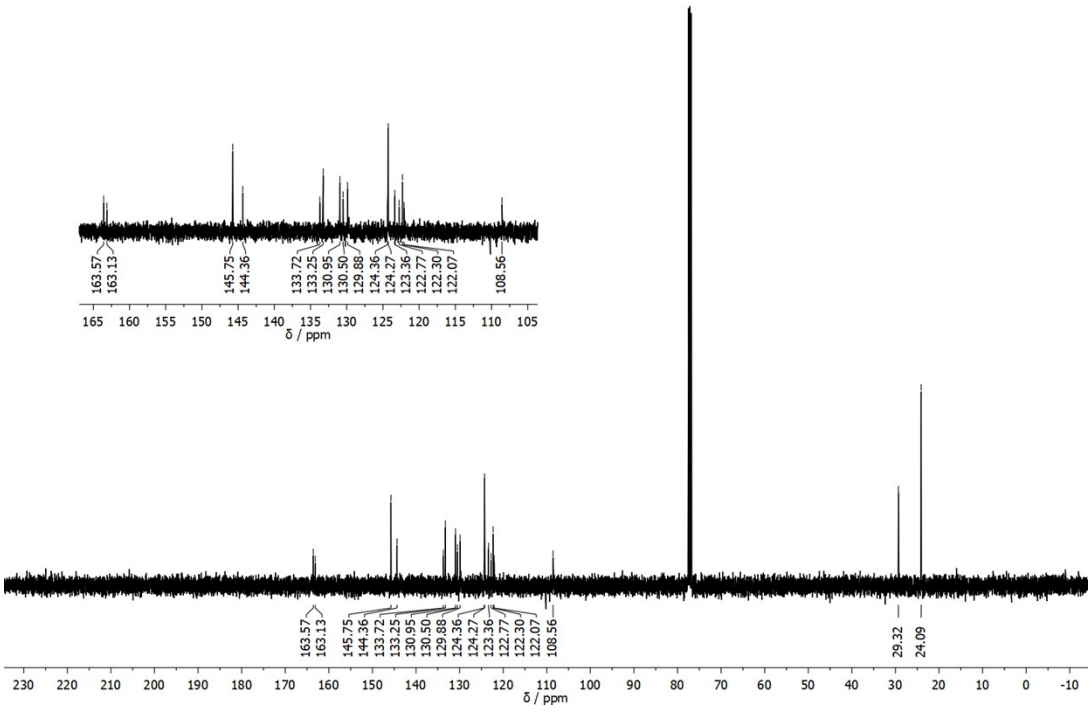

Figure S26. 101 MHz ^{13}C NMR of **10** in $CDCl_3$.

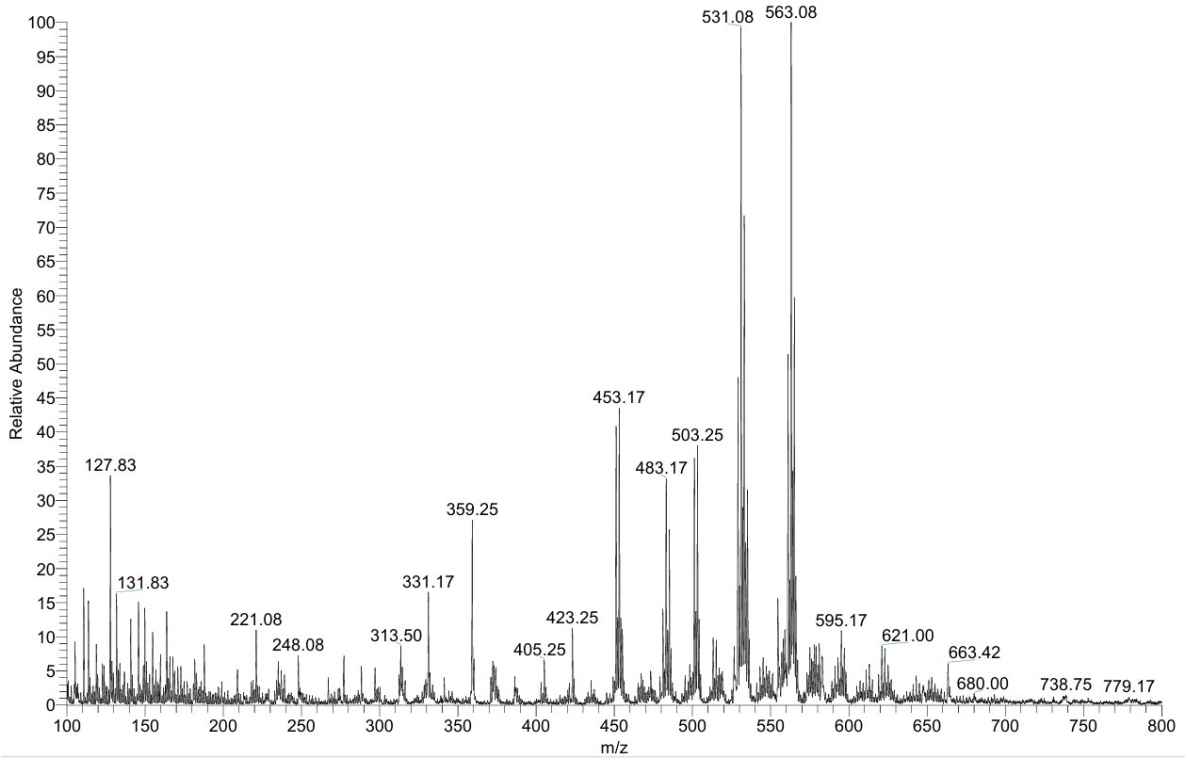

Figure S27. ESI-LRMS of **10**.

4 UV-Vis and electrochemistry studies

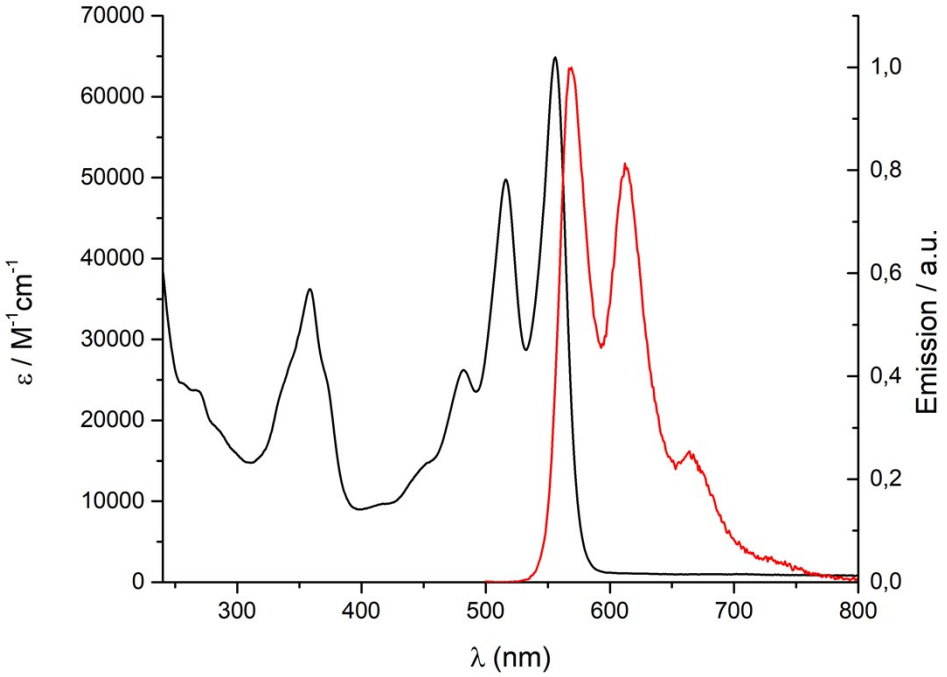

Figure S28. Absorption (black) and emission (red, λ_{ex}= 375 nm) spectra of **1** in $CHCl_3$.

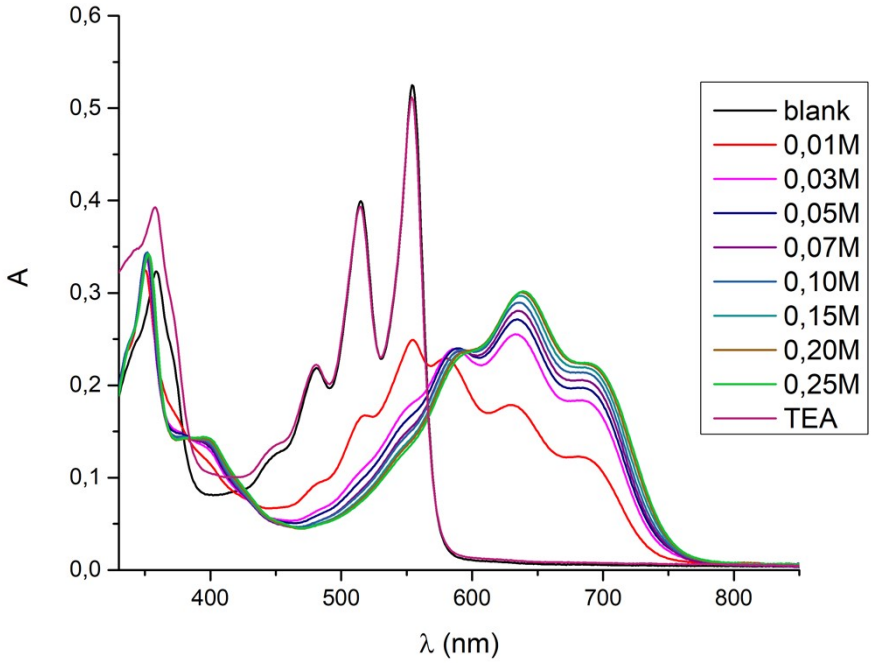

Figure S29. Absorption of **1** [7.3x10^{-6} M] with increasing concentrations of TFA in CH_2Cl_2. Final point is obtained by adding an amount of TEA that results in a concentration [0.25 M] of base.

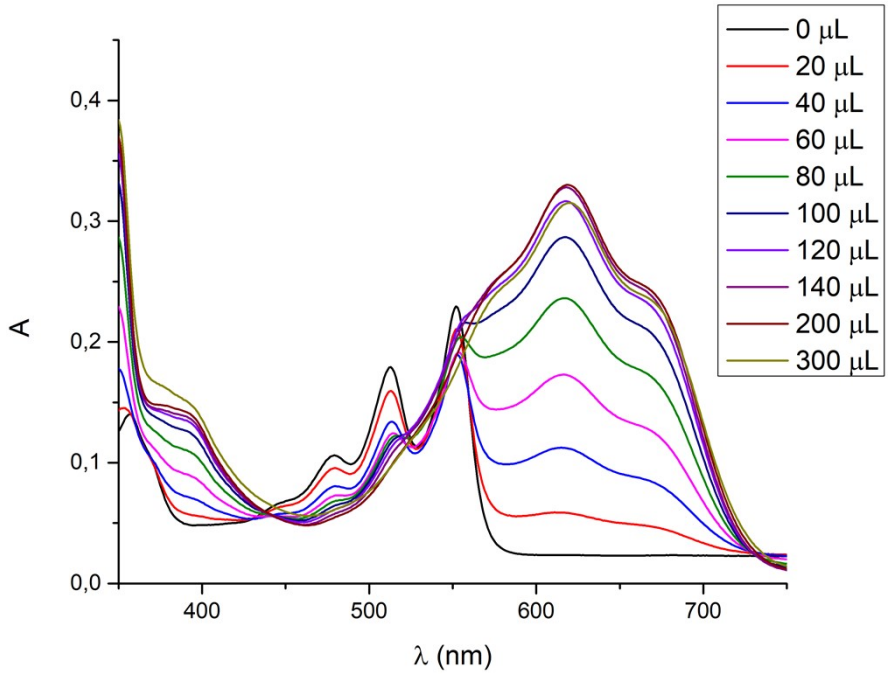

Figure S30. Absorption of **1** (1×10^{-5} M) in THF upon addition of increasing amounts of H_2SO_4.

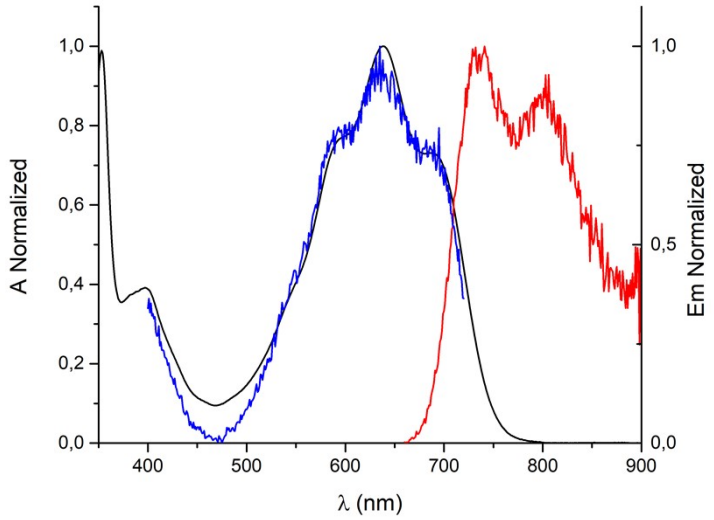

Figure S31. Absorption (black) and emission (red) of **1** in CH_2Cl_2 with 0.2 M TFA. Excitation spectra (blue) λ_{ex}= 734 nm is also reported.

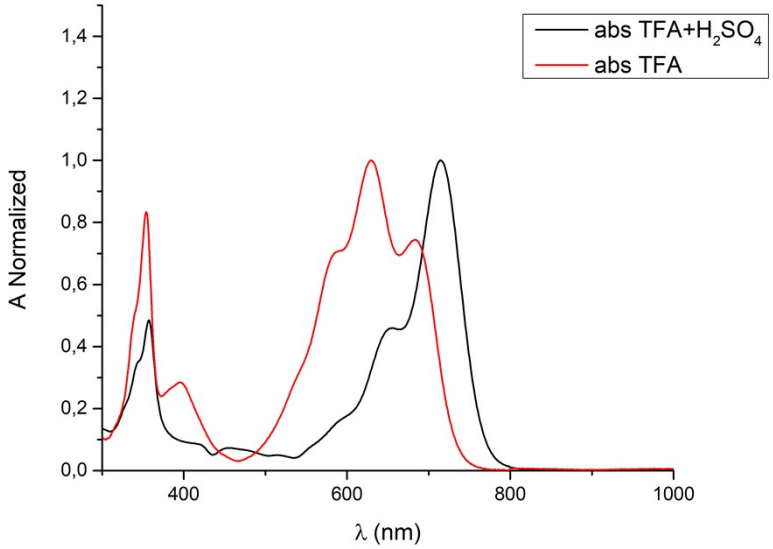

Figure S32. Absorption of **1** in TFA (red) and TFA with 0.2 M H_2SO_4 added (black).

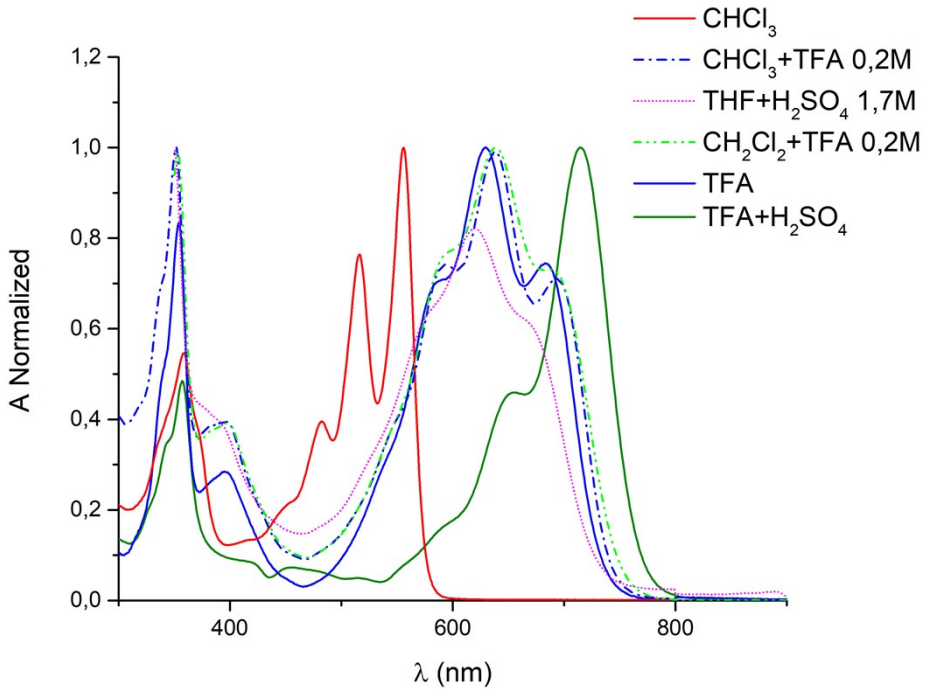

Figure S33. Absorption of **1** in different solvents and solvent/acid systems.

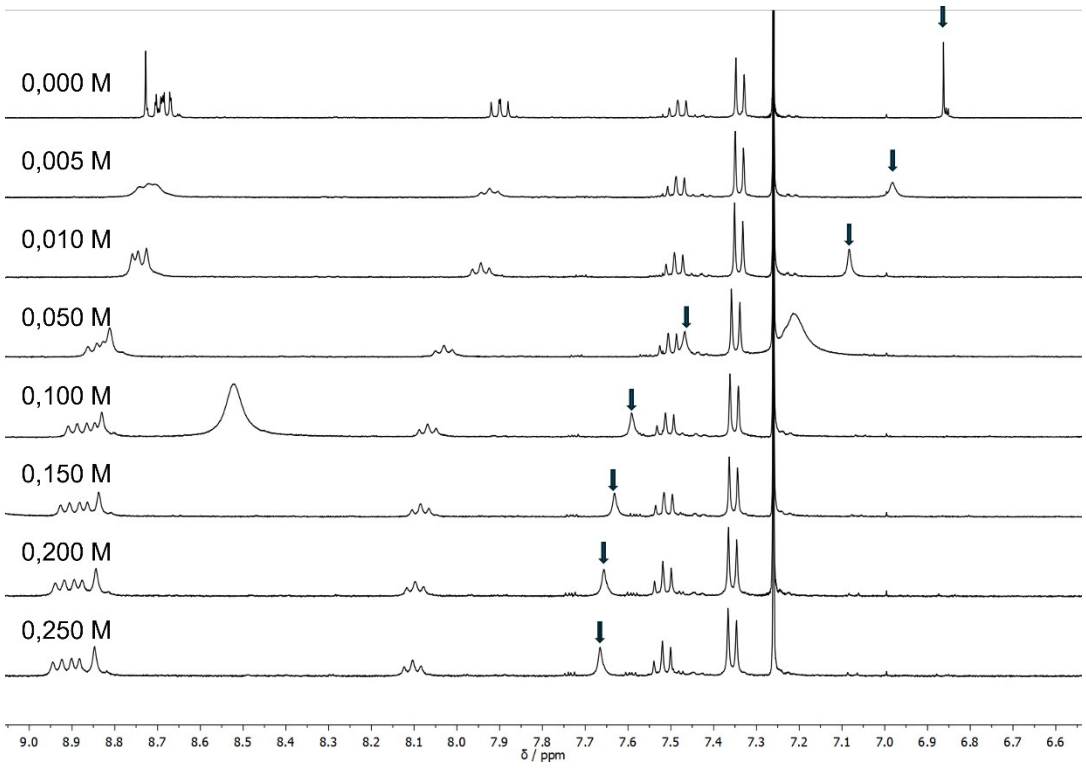

Figure S34. ^{1}H-NMR 400 MHz titration of **1** [3.2x10^{-3} M] in $CDCl_3$ with increasing concentrations of TFA. Diagnostic proton Ha is highlighted with the blue arrow.

5 Cyclic Voltammetry studies

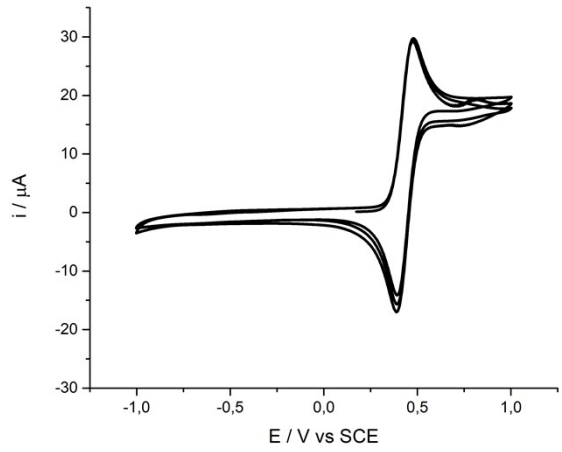

Figure S35. Cyclic voltammograms of **Fc** in CH_2Cl_2 as reference. Scan rates: 0.1 V s^{-1}. $TBAPF_6$ (0.1 M) is used as a supporting electrolyte E_{ox} Fc/Fc^+ = +0.43 V vs SCE.

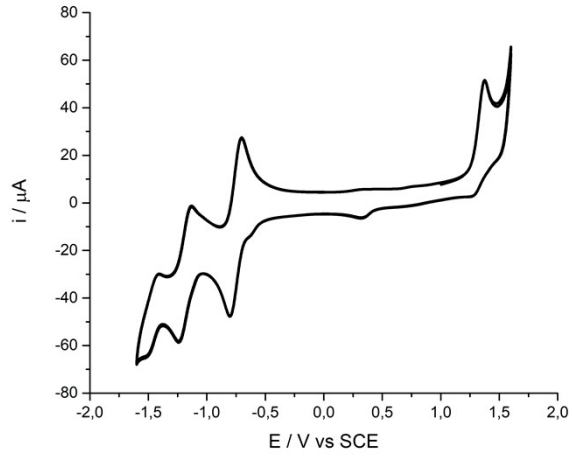

Figure S36. Cyclic voltammograms of **1** in CH_2Cl_2 (ca. 1 mM). Scan rates: 0.1 V s^{-1}. $TBAPF_6$ (0.1 M) is used as a supporting electrolyte.

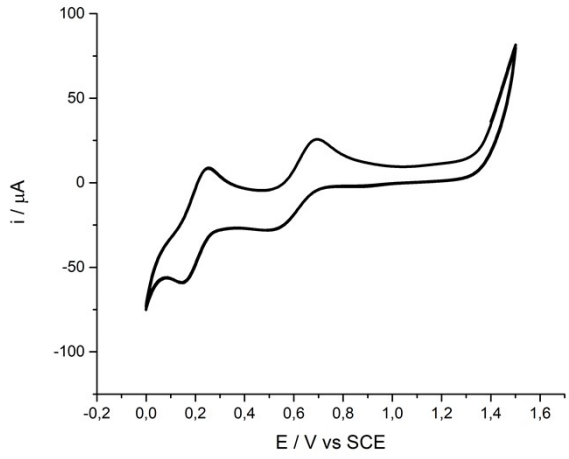

Figure S37. Cyclic voltammograms of **1** in CH_2Cl_2 (ca. 1 mM) containing 0.2 M TFA. Scan rates: 0.1 V s^{-1}. $TBAPF_6$ (0.1 M) is used as a supporting electrolyte.

6 Computational, Raman and two-dimensional electronic spectra

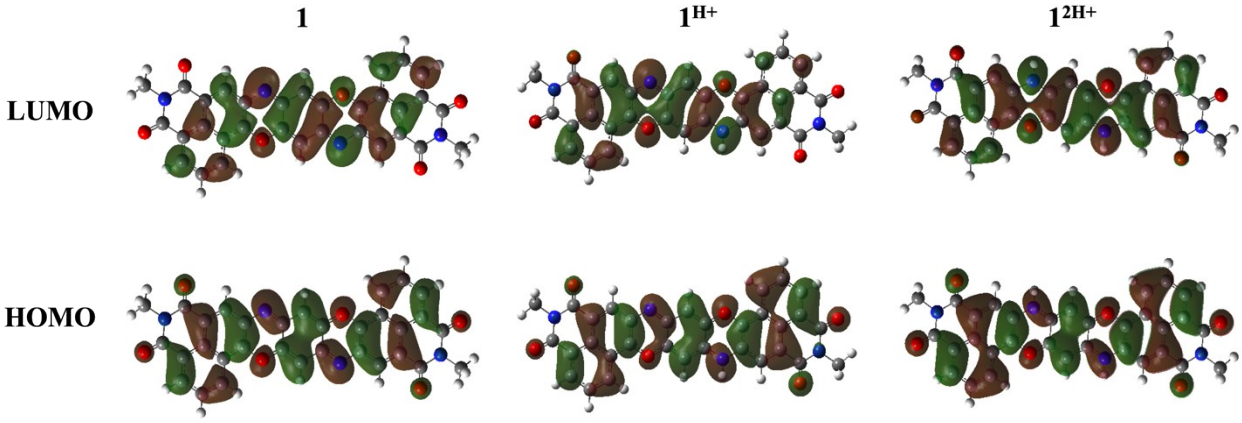

Figure S38. HOMO and LUMO molecular orbitals (MOs) attributable to the S_1 state for **1**, $\mathbf{1}^{1H+}$ and $\mathbf{1}^{2H+}$.

HOMO **1**	-6.70452 eV
LUMO **1**	-2.13062 eV
HOMO $\mathbf{1}^{H+}$	-7.63214 eV
LUMO $\mathbf{1}^{H+}$	-3.48301 eV
HOMO $\mathbf{1}^{2H+}$	-8.34425 eV
LUMO $\mathbf{1}^{2H+}$	-4.92057 eV

Table S1. Computed HOMO and LUMO values.

	Vertical exc. energy	Oscillator strength	Reorganization energy	Vertical em. energy	Reorganization energy (with scaled gradients)	Vertical em. energy (with scaled gradients)
1	2.48 eV / 499 nm	1.6526	0.33 eV	1.82 eV / 681 nm	0.19 eV	2.1 eV / 590 nm
$\mathbf{1}^{1H+}$	2.15 eV / 577 nm	1.5058	0.20 eV	1.75 eV / 708 nm	0.27 eV	1.61 eV / 770 nm
$\mathbf{1}^{2H+}$	1.61 eV / 767 nm	1.5983	0.18 eV	1.25 eV / 992 nm	0.10 eV	1.41 eV / 879 nm

Table S2. Computed vertical excitation energies, oscillator strengths, reorganization energies and vertical emission energies for **1**, $\mathbf{1}^{1H+}$ and $\mathbf{1}^{2H+}$. To match experimental vibronic structure, we applied a broadening factor of 300 cm^{-1} and scaling factors to S_1 energy gradients; in particular a scaling factor of 0.75 was applied to **1** and $\mathbf{1}^{2H+}$ while a scaling factor of 1.15 was applied to $\mathbf{1}^{H+}$ (Figure 2b of the main text).

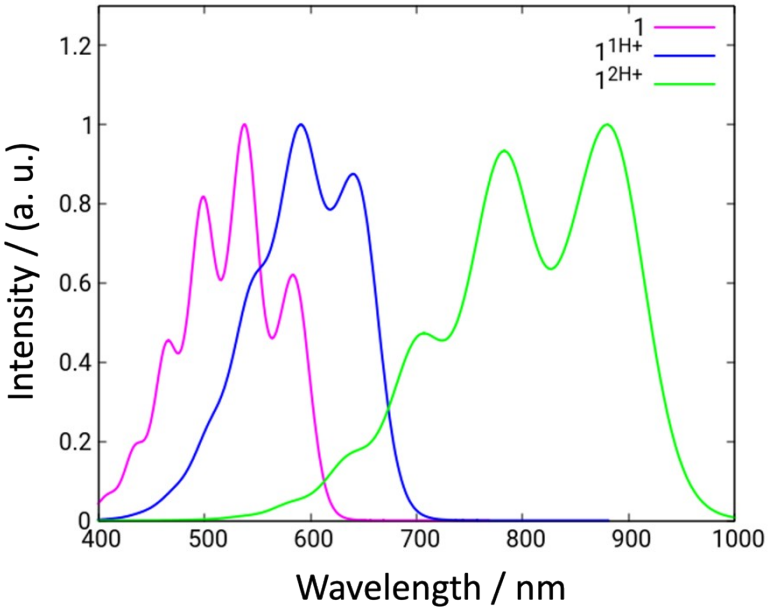

Figure S39. Computed vibronic spectra for **1**, $\mathbf{1}^{1H+}$ and $\mathbf{1}^{2H+}$ without scaling factors.

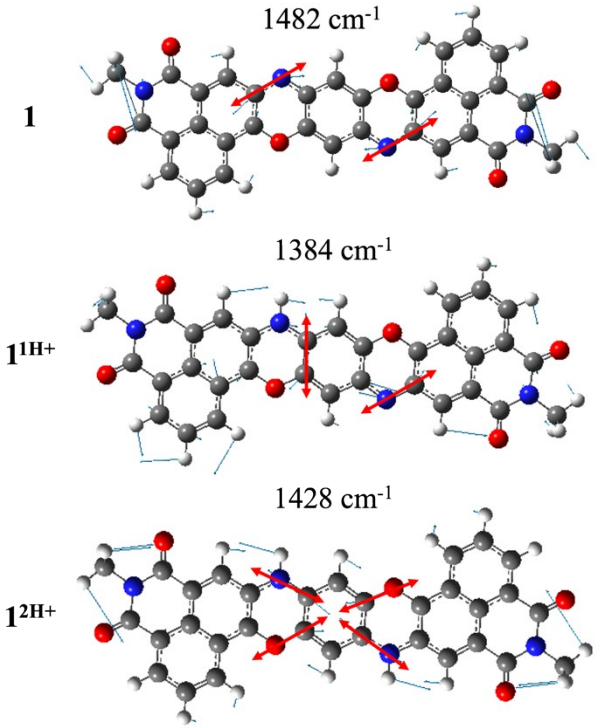

Figure S40. Dominant modes, highlighted with red double arrows only for the central aromatic core, which give rise to vibronic structure for **1**, $\mathbf{1}^{1H+}$, $\mathbf{1}^{2H+}$.

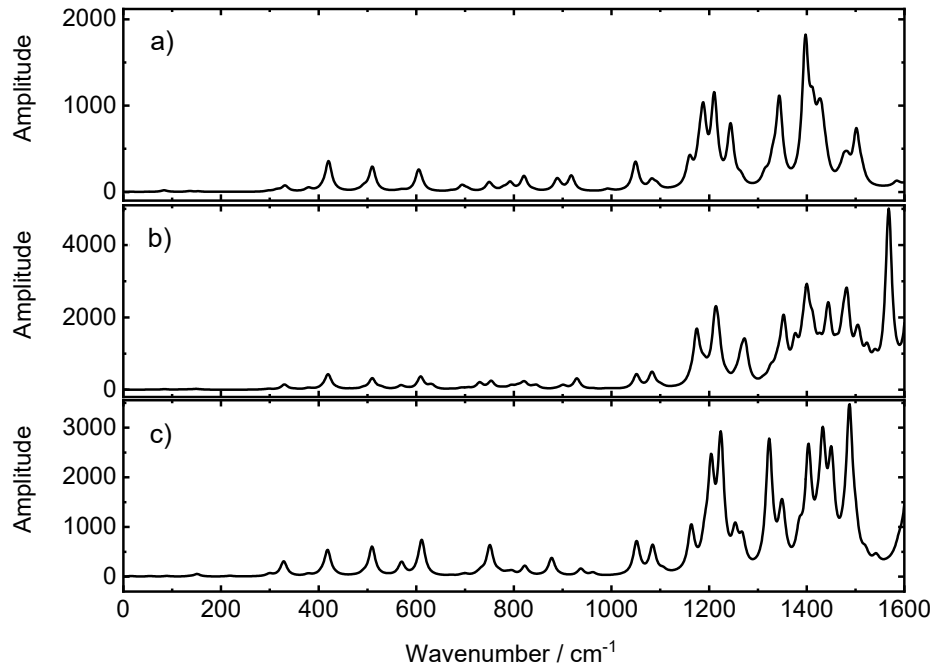

Figure S41. Calculated vibrational spectra on the S_0 state for **1** (a), $\mathbf{1}^{\mathbf{1H+}}$ (b) and $\mathbf{1}^{\mathbf{2H+}}$ (c).

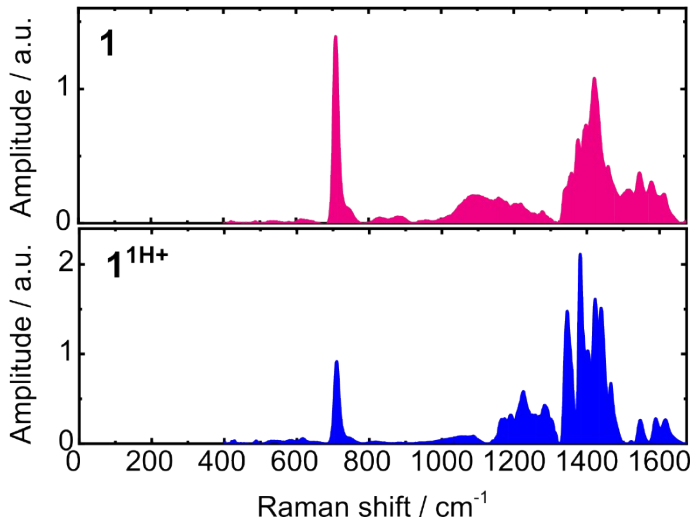

Figure S42. Raman spectra derived from CARS spectra after removal of the non-resonant background showing ground state vibrational frequencies for **1** (top) and $\mathbf{1}^{\mathbf{1H+}}$ (bottom). The peak at 700 cm^{-1} is attributed to the dichloromethane solvent. It was not possible to measure the Raman shift spectrum for $\mathbf{1}^{\mathbf{2H+}}$ due to experimental limitations, but this has no bearing on the interpretation of results. All five ground state vibrational spectra (computational spectra for **1**, $\mathbf{1}^{\mathbf{1H+}}$ and $\mathbf{1}^{\mathbf{2H+}}$ as well as Raman spectra for **1** and $\mathbf{1}^{\mathbf{1H+}}$) reveal a dense manifold of high-frequency vibrations, suggesting that the same would be observed via Raman spectroscopy of $\mathbf{1}^{\mathbf{2H+}}$.

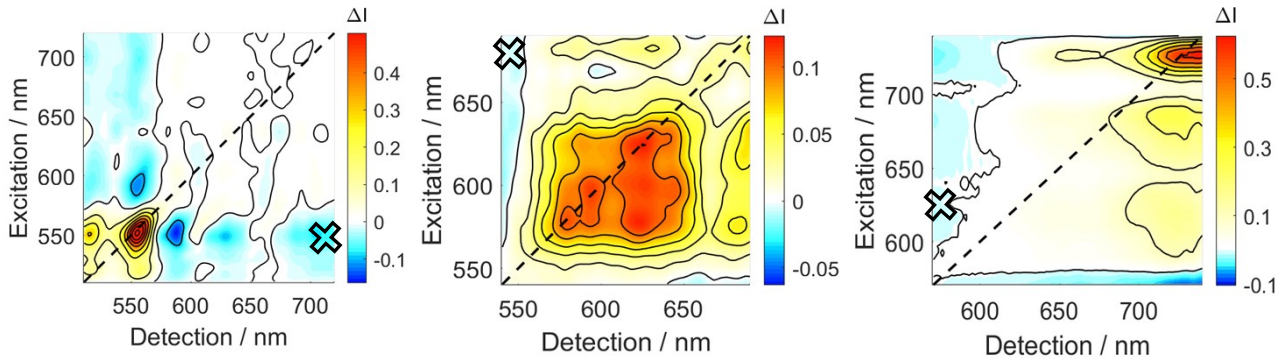

Figure S43. Two-dimensional electronic spectra for **1** (left), $\mathbf{1}^{\mathbf{1H+}}$ (middle) and $\mathbf{1}^{\mathbf{2H+}}$ (right) at t_2 = 100 fs. Positive peaks arise from ground state bleach and stimulated emission features while negative signals arise from excited state absorption. Black crosses on each map denote the point on the map for which kinetics were extracted for Fourier transformation to give the impulsive S_1 vibrational spectra in Figure 4.

S_0 minimum **1**

C	-7.231789	1.148653	-0.001154
C	-7.292177	2.526197	-0.001364
C	-5.982281	0.490187	-0.001251
C	-6.109344	3.291466	-0.001669
C	-4.879792	2.674532	-0.001763
C	-4.792814	1.260764	-0.001558
C	-5.917384	-0.927064	-0.001036
C	-4.701906	-1.564420	-0.001127
C	-3.495030	-0.827081	-0.001425
C	-3.560999	0.558107	-0.001627
C	-8.491931	0.364706	-0.000818
C	-7.163055	-1.725129	-0.000710
N	-8.369991	-1.026253	-0.000610
O	-9.585222	0.901359	-0.000764
O	-7.166285	-2.943196	-0.000560
O	-2.425872	1.304273	-0.001913
N	-2.283856	-1.505819	-0.001510
C	-1.218445	0.677350	-0.001776
C	-1.201686	-0.788816	-0.001678
C	-0.093323	1.422499	-0.001769
C	1.201682	0.788831	-0.001719
C	1.218441	-0.677335	-0.001738
C	0.093320	-1.422483	-0.001696
N	2.283853	1.505835	-0.001588
O	2.425868	-1.304258	-0.001839
C	3.495027	0.827096	-0.001463
C	3.560996	-0.558092	-0.001586
C	4.701902	1.564435	-0.001206
C	5.917381	0.927078	-0.001068
C	5.982276	-0.490172	-0.001186
C	4.792810	-1.260750	-0.001463
C	4.879789	-2.674518	-0.001582
C	6.109341	-3.291451	-0.001425

C	7.292174	-2.526182	-0.001131
C	7.231784	-1.148638	-0.001012
C	7.163051	1.725144	-0.000803
C	8.491926	-0.364693	-0.000673
O	7.166276	2.943212	-0.000719
O	9.585210	-0.901359	-0.000470
N	8.369986	1.026269	-0.000596
H	-8.271140	3.004827	-0.001284
H	-6.172428	4.379912	-0.001828
H	-3.962034	3.261478	-0.001998
H	-4.652141	-2.652809	-0.000964
H	-0.134687	2.510592	-0.001798
H	0.134683	-2.510576	-0.001668
H	4.652137	2.652825	-0.001120
H	3.962031	-3.261464	-0.001801
H	6.172426	-4.379897	-0.001520
H	8.271138	-3.004812	-0.000984
C	9.584906	1.837556	-0.000310
H	9.605201	2.480769	-0.889568
H	9.605042	2.480426	0.889200
H	10.440722	1.158991	-0.000350
C	-9.584912	-1.837537	-0.000309
H	-9.605271	-2.480696	-0.889607
H	-9.604989	-2.480463	0.889160
H	-10.440726	-1.158969	-0.000267

S_1 minimum **1**

C	-7.219869	1.142474	-0.001097
C	-7.277975	2.525381	-0.001215
C	-5.979201	0.482785	-0.001119
C	-6.094191	3.284792	-0.001331
C	-4.865406	2.663054	-0.001341
C	-4.781447	1.247196	-0.001240
C	-5.917731	-0.941156	-0.001042
C	-4.714340	-1.587712	-0.001087
C	-3.480557	-0.865835	-0.001187
C	-3.553701	0.550016	-0.001262
C	-8.485469	0.365239	-0.000930
C	-7.171518	-1.732105	-0.000927
N	-8.373223	-1.026307	-0.000978
O	-9.574390	0.909563	-0.001235
O	-7.180429	-2.949541	-0.001134
O	-2.425293	1.288622	-0.001375
N	-2.315498	-1.537670	-0.001211
C	-1.216576	0.639839	-0.001351
C	-1.193409	-0.787140	-0.001279
C	-0.079895	1.408223	-0.001398
C	1.193405	0.787156	-0.001375
C	1.216572	-0.639824	-0.001320
C	0.079891	-1.408208	-0.001274
N	2.315494	1.537686	-0.001397
O	2.425289	-1.288607	-0.001311

C	3.480553	0.865850	-0.001337
C	3.553697	-0.550001	-0.001287
C	4.714336	1.587727	-0.001318
C	5.917727	0.941171	-0.001252
C	5.979196	-0.482770	-0.001186
C	4.781442	-1.247181	-0.001215
C	4.865402	-2.663039	-0.001163
C	6.094186	-3.284777	-0.001073
C	7.277971	-2.525366	-0.001024
C	7.219864	-1.142459	-0.001081
C	7.171514	1.732120	-0.001272
C	8.485465	-0.365225	-0.000992
O	7.180425	2.949556	-0.001118
O	9.574385	-0.909550	-0.000852
N	8.373218	1.026322	-0.001075
H	-8.255960	3.005744	-0.001195
H	-6.152379	4.373606	-0.001413
H	-3.946358	3.248020	-0.001435
H	-4.673463	-2.676378	-0.001033
H	-0.138524	2.495754	-0.001444
H	0.138520	-2.495739	-0.001224
H	4.673459	2.676393	-0.001369
H	3.946353	-3.248005	-0.001191
H	6.152374	-4.373591	-0.001029
H	8.255955	-3.005729	-0.000937
C	9.593532	1.829851	-0.000946
H	9.617638	2.472598	-0.890418
H	9.617514	2.472527	0.888583
H	10.445016	1.145863	-0.000905
C	-9.593537	-1.829836	-0.001092
H	-9.617538	-2.472497	-0.890629
H	-9.617625	-2.472596	0.888372
H	-10.445020	-1.145847	-0.001096

S_0 minimum $\mathbf{1}^{\mathbf{1H+}}$

C	7.237291	-1.128524	0.000084
C	7.305674	-2.508340	0.000459
C	5.987007	-0.482343	-0.000022
C	6.131700	-3.282736	0.000714
C	4.896369	-2.675056	0.000624
C	4.806073	-1.263898	0.000266
C	5.919265	0.943211	-0.000385
C	4.716337	1.585259	-0.000432
C	3.505358	0.836619	-0.000141
C	3.575439	-0.559134	0.000185
C	8.496771	-0.339325	-0.000199
C	7.170544	1.745424	-0.000718
N	8.374684	1.051724	-0.000856
O	9.587215	-0.877143	0.000094
O	7.159213	2.961707	-0.000891
O	2.439197	-1.284654	0.000457
N	2.309111	1.488340	-0.000183
C	1.249684	-0.676296	0.000413

C	1.214068	0.770251	0.000079
C	0.113562	-1.445826	0.000650
C	-1.132076	-0.800661	0.000601
C	-1.196589	0.649962	0.000279
C	-0.073318	1.401610	0.000030
N	-2.282299	-1.474496	0.000808
O	-2.406618	1.274394	0.000301
C	-3.530470	-0.837738	0.000566
C	-3.557945	0.541480	0.000318
C	-4.726597	-1.575633	0.000496
C	-5.931661	-0.916645	0.000230
C	-5.978227	0.497207	0.000035
C	-4.779586	1.254339	0.000074
C	-4.849700	2.670587	-0.000120
C	-6.072518	3.297332	-0.000334
C	-7.265676	2.544531	-0.000381
C	-7.221948	1.168083	-0.000209
C	-7.186235	-1.704928	0.000092
C	-8.490085	0.395820	-0.000304
O	-7.189505	-2.923034	0.000177
O	-9.576637	0.943144	-0.000451
N	-8.383144	-0.997919	-0.000219
H	8.287722	-2.980466	0.000548
H	6.203415	-4.370209	0.000989
H	3.983787	-3.269932	0.000828
H	4.664289	2.672987	-0.000691
H	0.184342	-2.532867	0.000814
H	-0.124143	2.488993	-0.000182
H	-4.712326	-2.666032	0.000632
H	-3.926886	3.249061	-0.000090
H	-6.125148	4.386123	-0.000473
H	-8.237705	3.036897	-0.000557
C	-9.606903	-1.797555	-0.000382
H	-9.633688	-2.438400	-0.890979
H	-9.633172	-2.439457	0.889450
H	-10.455961	-1.110796	0.000224
C	9.589861	1.865276	-0.001258
H	9.607554	2.507085	-0.891242
H	9.609021	2.506005	0.889496
H	10.446740	1.188385	-0.002303
H	-2.262055	-2.490318	0.001315

S_1 minimum $\mathbf{1}^{\mathbf{1H+}}$

C	7.238871	-1.115644	-0.000052
C	7.309067	-2.499712	0.000292
C	5.993274	-0.470635	-0.000126
C	6.136331	-3.273743	0.000541
C	4.900815	-2.664867	0.000468
C	4.805788	-1.250013	0.000141
C	5.921191	0.954323	-0.000435
C	4.714141	1.590766	-0.000475
C	3.493401	0.852620	-0.000238

C	3.573858	-0.563756	0.000068
C	8.498737	-0.326677	-0.000363
C	7.170002	1.756860	-0.000684
N	8.376090	1.063215	-0.000624
O	9.589253	-0.865604	0.000118
O	7.161119	2.973627	-0.000604
O	2.451713	-1.308222	0.000313
N	2.318326	1.513881	-0.000305
C	1.243599	-0.669248	0.000236
C	1.207040	0.755861	-0.000077
C	0.109667	-1.449970	0.000456
C	-1.138511	-0.817749	0.000373
C	-1.197500	0.599163	0.000065
C	-0.066314	1.373390	-0.000151
N	-2.322472	-1.514943	0.000541
O	-2.408711	1.236749	-0.000023
C	-3.528729	-0.885125	0.000362
C	-3.549348	0.525247	0.000073
C	-4.747408	-1.602289	0.000456
C	-5.936311	-0.926242	0.000279
C	-5.972913	0.496020	-0.000016
C	-4.767300	1.242760	-0.000101
C	-4.825390	2.657505	-0.000343
C	-6.047101	3.295235	-0.000514
C	-7.240546	2.553215	-0.000471
C	-7.204823	1.169462	-0.000236
C	-7.204289	-1.702988	0.000482
C	-8.482429	0.408813	-0.000330
O	-7.211965	-2.919576	0.000366
O	-9.559751	0.970747	-0.000328
N	-8.391785	-0.985477	0.000118
H	8.292063	-2.970018	0.000339
H	6.207599	-4.361327	0.000792
H	3.988040	-3.259375	0.000666
H	4.660929	2.678548	-0.000698
H	0.193568	-2.536377	0.000673
H	-0.133847	2.459945	-0.000385
H	-4.747608	-2.692476	0.000684
H	-3.899362	3.230741	-0.000390
H	-6.090208	4.384249	-0.000705
H	-8.210163	3.050089	-0.000651
C	-9.624720	-1.772479	0.000156
H	-9.657098	-2.412534	-0.890649
H	-9.656813	-2.412806	0.890765
H	-10.466517	-1.076884	0.000361
C	9.590563	1.877386	-0.000670
H	9.608399	2.519348	-0.890594
H	9.609231	2.518368	0.889960
H	10.447977	1.201096	-0.001392
H	-2.298249	-2.530998	0.000812

S_0 minimum $\mathbf{1}^{2H+}$

C	-7.224019	1.142964	0.000164
C	-7.278764	2.521047	-0.032926

C	-5.978075	0.486550	-0.007930
C	-6.095334	3.284170	-0.074922
C	-4.865341	2.669327	-0.082430
C	-4.788062	1.255943	-0.048943
C	-5.924155	-0.932978	0.025531
C	-4.727854	-1.594693	0.016370
C	-3.533605	-0.844963	-0.023788
C	-3.568823	0.541665	-0.052530
C	-8.489709	0.363023	0.045757
C	-7.181168	-1.729110	0.071865
N	-8.377687	-1.030157	0.079601
O	-9.574211	0.908908	0.053845
O	-7.165428	-2.944581	0.102203
O	-2.413820	1.256998	-0.083678
N	-2.291045	-1.457391	-0.037247
C	-1.219292	0.661153	-0.077123
C	-1.145899	-0.792773	-0.064920
C	-0.095288	1.432587	-0.078164
C	1.160081	0.793341	-0.064923
C	1.233473	-0.660587	-0.077059
C	0.109469	-1.432020	-0.078098
N	2.305225	1.457957	-0.037249
O	2.427999	-1.256433	-0.083554
C	3.547784	0.845529	-0.023741
C	3.583003	-0.541100	-0.052419
C	4.742035	1.595260	0.016388
C	5.938335	0.933544	0.025593
C	5.992252	-0.485986	-0.007791
C	4.802240	-1.255379	-0.048779
C	4.879516	-2.668765	-0.082191
C	6.109507	-3.283611	-0.074633
C	7.292938	-2.520487	-0.032656
C	7.238195	-1.142402	0.000357
C	7.195350	1.729677	0.071881
C	8.503886	-0.362460	0.045927
O	7.179604	2.945151	0.102125
O	9.588387	-0.908346	0.054096
N	8.391868	1.030722	0.079668
H	-8.255147	3.004639	-0.025489
H	-6.158695	4.371762	-0.101115
H	-3.949083	3.257249	-0.113945
H	-4.710886	-2.684437	0.040433
H	-0.176645	2.518919	-0.084092
H	0.190830	-2.518353	-0.083967
H	4.725070	2.685006	0.040388
H	3.963255	-3.256685	-0.113688
H	6.172868	-4.371204	-0.100768
H	8.269319	-3.004082	-0.025172
C	9.612736	1.835918	0.126841
H	9.653628	2.499234	-0.746297
H	9.615371	2.452747	1.034341
H	10.464975	1.153276	0.127280
C	-9.598545	-1.835363	0.126834
H	-9.639560	-2.498564	-0.746387
H	-9.601045	-2.452310	1.034251
H	-10.450788	-1.152725	0.127469

H	2.279848	2.478480	-0.017703
H	-2.265655	-2.477912	-0.017681

S_1 minimum $\mathbf{1}^{2H+}$

C	-7.219963	1.137184	0.012760
C	-7.271524	2.523577	-0.015550
C	-5.982984	0.479668	-0.005284
C	-6.090398	3.279764	-0.062231
C	-4.859730	2.656142	-0.079392
C	-4.786366	1.241956	-0.051131
C	-5.932585	-0.941499	0.023525
C	-4.736217	-1.608106	0.004580
C	-3.534142	-0.876149	-0.041491
C	-3.566860	0.536006	-0.064832
C	-8.490808	0.363368	0.063778
C	-7.192919	-1.732386	0.075579
N	-8.386650	-1.028726	0.092317
O	-9.569609	0.919540	0.080119
O	-7.179635	-2.947640	0.102538
O	-2.427919	1.250452	-0.100628
N	-2.313954	-1.491578	-0.064389
C	-1.220182	0.627286	-0.099149
C	-1.146834	-0.791419	-0.090366
C	-0.092437	1.414704	-0.100481
C	1.161016	0.791978	-0.090397
C	1.234364	-0.626727	-0.099074
C	0.106619	-1.414146	-0.100372
N	2.328135	1.492139	-0.064434
O	2.442101	-1.249894	-0.100481
C	3.548323	0.876710	-0.041472
C	3.581042	-0.535446	-0.064722
C	4.750398	1.608669	0.004580
C	5.946765	0.942063	0.023585
C	5.997165	-0.479105	-0.005148
C	4.800546	-1.241396	-0.050970
C	4.873911	-2.655583	-0.079161
C	6.104579	-3.279204	-0.061961
C	7.285704	-2.523016	-0.015304
C	7.234143	-1.136622	0.012942
C	7.207098	1.732952	0.075627
C	8.504988	-0.362803	0.063939
O	7.193814	2.948207	0.102515
O	9.583788	-0.918974	0.080307
N	8.400829	1.029293	0.092394
H	-8.247483	3.007987	-0.000232
H	-6.147171	4.367725	-0.084397
H	-3.941788	3.241310	-0.114370
H	-4.725626	-2.698000	0.025641
H	-0.189038	2.499645	-0.102902
H	0.203221	-2.499086	-0.102705
H	4.739809	2.698564	0.025582
H	3.955969	-3.240753	-0.114122
H	6.161352	-4.367167	-0.084079
H	8.261663	-3.007424	0.000046
C	9.625438	1.829300	0.144170

H	9.673847	2.489097	-0.731178
H	9.624910	2.448617	1.049893
H	10.474746	1.143032	0.151852
C	-9.611259	-1.828730	0.144131
H	-9.659730	-2.488484	-0.731246
H	-9.610672	-2.448090	1.049823
H	-10.460563	-1.142459	0.151897
H	2.295004	2.509760	-0.047686
H	-2.280824	-2.509198	-0.047578

Energy gap law calculations

Table S3. Experimentally determined S_1 decay rate, equal to the sum of radiative and nonradiative decay rates ($k_r + k_{nr}$), and fluorescence quantum yield (Φ_f), which together with equation S1 (below) gives the rate of nonradiative decay k_{nr}. Experimentally determined S_0-S_1 energy gap values, ΔE, theoretically determined dominant vibrational frequencies, ω_{theory}, and experimentally determined vibrational frequencies, ω_{exp}, are used to benchmark the trend in results against the Energy Gap Law.

Molecule	Exp. rate / s^{-1}	Φ_f / a.u.	k_{nr} / s^{-1}	ΔE / nm	ΔE / eV	ω_{theory} / cm^{-1}	ω_{exp} / cm^{-1}
1	$8.33x10^8$	0.7	$2.50x10^8$	554	2.24	1482	1432
$\mathbf{1}^{1H+}$	$1.09x10^{10}$	< 0.01	$1.08x10^{10}$	693	1.79	1384	1354
$\mathbf{1}^{2H+}$	$3.70x10^{10}$	0	$3.70x10^{10}$	715	1.73	1428	1426

$$\Phi_f = \frac{k_r}{k_r + k_{nr}} \quad \text{(S1)}$$

7 X-Ray diffraction

Data collections for **1**, **1Br** and **1•TFA** were performed at the XRD2 beamline of the Elettra Synchrotron, Trieste (Italy).[5] The crystals were dipped in NHV oil (Jena Bioscience, Jena, Germany) and mounted on the goniometer head with kapton loops (MiTeGen, Ithaca, USA). Complete datasets were collected at 100 K or 298 K (nitrogen stream supplied through an Oxford Cryostream 700) through the rotating crystal method. Data were acquired using monochromatic wavelength of 0.620 Å on a Pilatus 6M hybrid-pixel area detector (DECTRIS Ltd., Baden-Daettwil, Switzerland). The diffraction data were indexed, integrated and scaled using XDS.[6] Partial datasets, from randomly orientated crystals, have been merged with CCP4-Aimless code[7,8] to obtain complete sets of data for **1•TFA** triclinic polymorph (α). An alternative **1•TFA** monoclinic polymorph (β) has been found but its crystals diffracted to a maximum resolution of ~1.0 Å. The structures were solved by the dual space algorithm implemented in the SHELXT code.[9] Fourier analysis and refinement were performed by the full-matrix least-squares methods based on F^2 implemented in SHELXL (Version 2018/3).[10] The Coot program was used for modeling.[11] Anisotropic thermal motion refinement have been used for all phenoxazine based moieties in all structures but **1•TFA** polymorph β, where only heteroatoms have been treated anisotropically to avoid overrefinement. Geometry and thermal motion parameters restrains (SIMU, DFIX, DANG and SAME) have been used on disordered molecules. Hydrogen atoms were included at calculated positions with isotropic $U_{factors} = 1.2 \bullet U_{eq}$ or $U_{factors} = 1.5 \bullet U_{eq}$ for methyl and hydroxyl groups (U_{eq} being the equivalent isotropic thermal factor of the bonded non hydrogen atom). Hydrogen atoms for water

molecules have not been included in the refined models since it was not possible to locate them unambiguously in electron-density peaks of Fourier difference maps. Pictures were prepared using Ortep-3[12], CCDC Mercury[13] and Pymol[14] software. Essential crystal and refinement data are reported below (Table S3 - contribution of unmodeled atoms in disordered solvent is accounted therein).

Molecules have been crystallized in centrosymmetric space groups with half TPDO diimide molecule in the crystallographic asymmetric unit (ASU - Figure S44). Molecules barycenter lay on crystallographic inversion centers. Only **1•TFA** polymorph β crystal form bears a complete molecular entity in the ASU. TPDO diimide cores are almost flat (distance of core atoms from the mean plane are d < 0.18 Å) and perfectly superimposable, with minor dipp side chains rearrangements and negligible differences in bond distances (Figure S45).

All the hydrogens have been placed in calculated positions and protonation state of **1•TFA** molecules have been assigned on the basis of additional experimental evidence reported in this work. Disorder on trifluoroacetate counter ions is consistent with the presence of distributed partial charges.

Crystal packing show extensive hydrophobic interactions with multiple CH•••π contacts but poor π•••π stacking (closer ring centroids at $d_{\pi\cdots\pi}$ > 4.3 Å, with ~4.5 Å slippage) due to steric hindrance of dipp groups. Free spaces available among phenoxazine diimide cores are filled up by solvent molecules (and counterions for **1•TFA**). Most of these molecules adopt multiple conformations unless they are involved in well oriented polar contacts with heteroatoms of the NDI scaffold. No phase transition has been found for **1** and **1•TFA** polymorph α crystals upon cooling from 298K to 100K (Table S4).

Table S4. Crystallographic data and refinement details for **1** (at 100K and 298K), **1Br** (at 100K), **1•TFA** polymorph α (at 100K and 298K) and **1•TFA** polymorph β (at 100K).

	1 at 100K	**1 at 298K**	**1Br at 100K**
CCDC Number	2383224	2383220	2383219
Chemical Formula	$C_{54}H_{44}N_4O_6$ $\cdot^7/_4CHCl_3\cdot^1/_3C_6H_{14}$	$C_{54}H_{44}N_4O_6$ $\cdot^4/_3CHCl_3\cdot^2/_3C_6H_{14}$	$C_{54}H_{42}Br_2N_4O_6$ $\cdot 4CHCl_3$
Formula weight	1073.71 g/mol	1060.43 g/mol	1480.21 g/mol
Temperature	100(2) K	298(2) K	100(2) K
Wavelength	0.620 Å	0.620 Å	0.620 Å
Crystal system	Monoclinic	Monoclinic	Monoclinic
Space Group	$P\,2_1/n$	$P\,2_1/n$	$P\,2_1/n$
Unit cell dimensions	a = 14.620(3) Å	a = 14.890(3) Å	a = 12.675(3) Å
	b = 9.322(2) Å	b = 9.385(2) Å	b = 10.178(2) Å
	c = 23.044(5) Å	c = 23.045(5) Å	c = 23.722(5) Å
	α = 90°	α = 90°	α = 90°
	β = 108.38(3)°	β = 108.74(3)°	β = 95.42(3)°
	γ = 90°	γ = 90°	γ = 90°
Volume	2980.3(11) Å^3	3049.8(12) Å^3	3046.6(11) Å^3
Z	2	2	2
Density (calculated)	1.196 g·cm^{-3}	1.155 g·cm^{-3}	1.614 g·cm^{-3}
Absorption coefficient	0.203 mm^{-1}	0.164 mm^{-1}	1.320 mm^{-1}
F(000)	1115	1109	1488
Theta range for data collection	1.7° to 25.5°	1.7° to 25.5°	1.6° to 31.1°
Index ranges	-19 ≤ h ≤ 19,	-19 ≤ h ≤ 19,	-21 ≤ h ≤ 21,
	-11 ≤ k ≤ 11,	-11 ≤ k ≤ 11,	-16 ≤ k ≤ 16,
	-26 ≤ l ≤ 26	-29 ≤ l ≤ 29	-39 ≤ l ≤ 39
Reflections collected	35022	41241	48017
Independent reflections (data with I>2σ(I))	6549 (2706)	6424 (2614)	13188 (6896)
Resolution	0.72 Å	0.78 Å	0.60 Å
Data multiplicity (max resltn)	4.10 (1.03)	5.95 (6.10)	3.20 (1.93)
I/σ(I) (max resltn)	6.15 (0.35)	5.18 (0.48)	9.07 (1.18)
R_{merge} (max resltn)	0.0807 (0.9572)	0.0923 (1.041)	0.0629 (0.5245)
Data completeness (max resltn)	78.4% (36.3%)	95.9% (94.8%)	89.5% (72.2%)
Refinement method	Full-matrix least-squares on F^2	Full-matrix least-squares on F^2	Full-matrix least-squares on F^2
Data / restraints / parameters	6549 / 37 / 409	6424 / 54 / 369	13188 / 6 / 391
Goodness-of-fit on F^2	1.067	1.097	1.025
Δ/σ_{max}	0.002	0.007	0.002
Final R indices [I>2σ(I)]	R_1 = 0.1234	R_1 = 0.1199	R_1 = 0.0663
	wR_2 = 0.2401	wR_2 = 0.2463	wR_2 = 0.1685
R indices (all data)	R_1 = 0.2172	R_1 = 0.1906	R_1 = 0.1342
	wR_2 = 0.2728	wR_2 = 0.2772	wR_2 = 0.2019
Largest diff. peak and hole	0.617 and -0.280 eÅ^{-3}	0.510 and -0.233 eÅ^{-3}	0.897 and -0.901 eÅ^{-3}
R.M.S. deviation from mean	0.065 eÅ^{-3}	0.059 eÅ^{-3}	0.095 eÅ^{-3}
Deviation from mean plane-	0.021(6) Å	0.021(6) Å	0.046(3) Å

$$R_1 = \Sigma\, ||Fo|-|Fc|| \,/\, \Sigma\, |Fo|,\; wR_2 = \{\Sigma\,[w(Fo^2 - F4\,)^2] \,/\, \Sigma\,[w(Fo^2\,)^2]\}^{½}$$

Table S4 (cont.). Crystallographic data and refinement details for **1** (at 100K and 298K), **1Br** (at 100K), **1•TFA** polymorph α (at 100K and 298K) and **1•TFA** polymorph β (at 100K).

	1•TFA α at 100K	**1•TFA α at 298K**	**1•TFA β at 100K**
CCDC Number	2383221	2383222	2383223
Chemical Formula	$[C_{54}H_{45}N_4O_6](C_2F_3O_2)$ $\cdot 5C_2HF_3O_2\cdot H_2O$	$[C_{54}H_{45}N_4O_6](C_2F_3O_2)$ $\cdot 5C_2HF_3O_2\cdot H_2O$	$[C_{54}H_{45}N_4O_6](C_2F_3O_2)$ $\cdot 2C_2HF_3O_2\cdot 3H_2O$
Formula weight	1547.11 g/mol	1547.11 g/mol	1241.06 g/mol
Temperature	100(2) K	298(2) K	100(2) K
Wavelength	0.620 Å	0.620 Å	0.620 Å
Crystal system	Triclinic	Triclinic	Monoclinic
Space Group	*P* -1	*P* -1	*C c*
Unit cell dimensions	*a* = 8.593(2) Å	*a* = 8.773(2) Å	*a* = 8.483(2) Å
	b = 9.152(2) Å	*b* = 9.322(2) Å	*b* = 16.394(3) Å
	c = 23.901(5) Å	*c* = 24.333(5) Å	*c* = 41.630(8) Å
	α = 88.57(3)°	*α* = 87.25(3)°	*α* = 90°
	β = 83.90(3)°	*β* = 81.84(3)°	*β* = 90.73(3)°
	γ = 63.20(3)°	*γ* = 62.29(3)°	*γ* = 90°
Volume	1667.7(7) Å^3	1743.5(8) Å^3	5789(2) Å^3
Z	1	1	4
Density (calculated)	1.540 g·cm^{-3}	1.473 g·cm^{-3}	1.424 g·cm^{-3}
Absorption coefficient	0.104 mm^{-1}	0.100 mm^{-1}	0.088 mm^{-1}
F(000)	790	790	2568
Theta range for data collection	2.2° to 29.0°	1.5° to 27.1°	1.7° to 16.8°
Index ranges	-13 ≤ h ≤ 13,	-12 ≤ h ≤ 12,	-7 ≤ h ≤ 7,
	-14 ≤ k ≤ 14,	-13 ≤ k ≤ 13,	-15 ≤ k ≤ 15,
	-37 ≤ l ≤ 37	-35 ≤ l ≤ 35	-38 ≤ l ≤ 38
Reflections collected	101359	68641	8701
Independent reflections (data with I>2σ(I))	13149 (10011)	11050 (7457)	4621 (1878)
Resolution	0.64 Å	0.68 Å	1.08 Å
Data multiplicity (max resltn)	7.61 (7.01)	5.93 (5.43)	3.51 (3.57)
I/σ(I) (max resltn)	14.84 (9.36)	6.40 (2.98)	6.21 (2.35)
R_{merge} (max resltn)	0.0879 (0.2443)	0.0796 (0.2886)	0.1441 (0.3835)
Data completeness (max resltn)	98.8% (98.2%)	95.5% (93.4%)	99.5% (99.7%)
Refinement method	Full-matrix least-squares on F^2	Full-matrix least-squares on F^2	Full-matrix least-squares on F^2
Data / restraints / parameters	13149 / 328 / 548	11050 / 162 / 488	4621 / 224 / 402
Goodness-of-fit on F^2	0.975	1.100	1.129
Δ/σ_{max}	0.012	0.029	0.000
Final R indices [I>2σ(I)]	R_1 = 0.1316	R_1 = 0.1208	R_1 = 0.1364
	wR_2 = 0.2547	wR_2 = 0.2872	wR_2 = 0.2512
R indices (all data)	R_1 = 0.1483	R_1 = 0.1437	R_1 = 0.2736
	wR_2 = 0.2610	wR_2 = 0.3000	wR_2 = 0.3120
Largest diff. peak and hole	0.874 and -0.820 eÅ^{-3}	0.618 and -0.410 eÅ^{-3}	0.477 and -0.423 eÅ^{-3}
R.M.S. deviation from mean	0.103 eÅ^{-3}	0.086 eÅ^{-3}	0.086 eÅ^{-3}
Deviation from mean plane	0.034(3) Å	0.058(3) Å	0.052(27) Å

$$R_1 = \Sigma \; ||Fo|-|Fc|| \; / \; \Sigma \; |Fo|, \; wR_2 = \{\Sigma \; [w(Fo^2 - F4\,)^2] \; / \; \Sigma \; [w(Fo^2\,)^2]\}^{½}$$

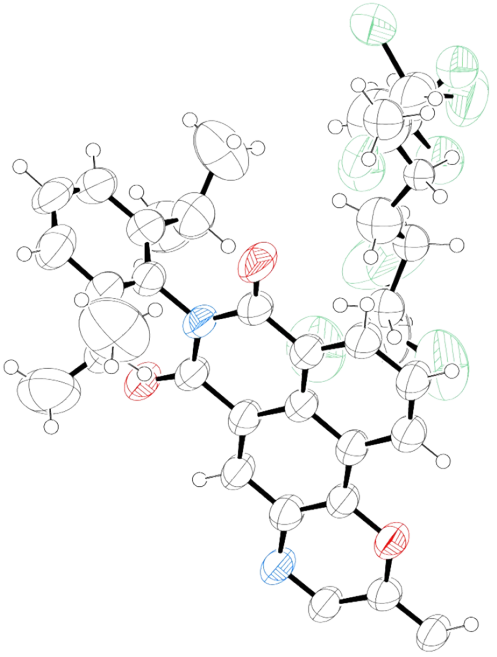

A)

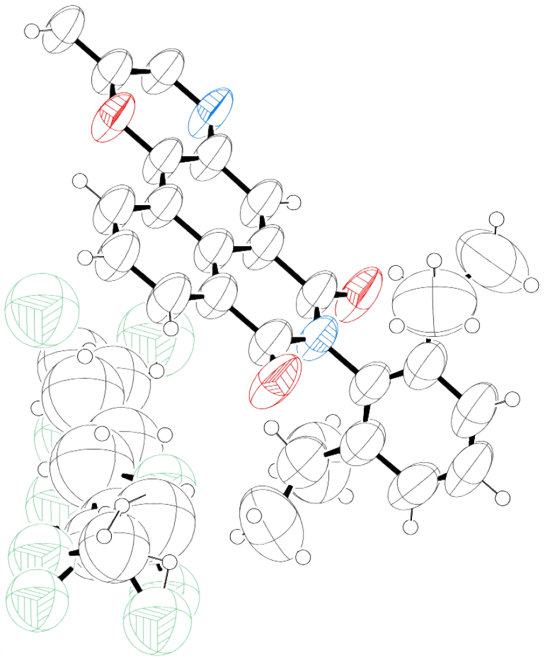

B)

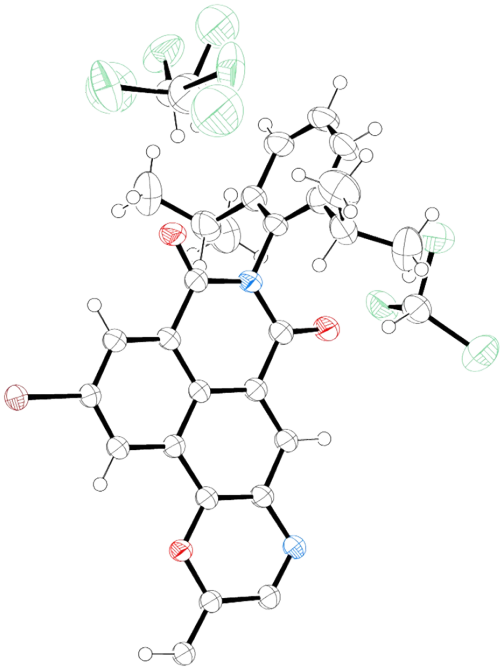

C)

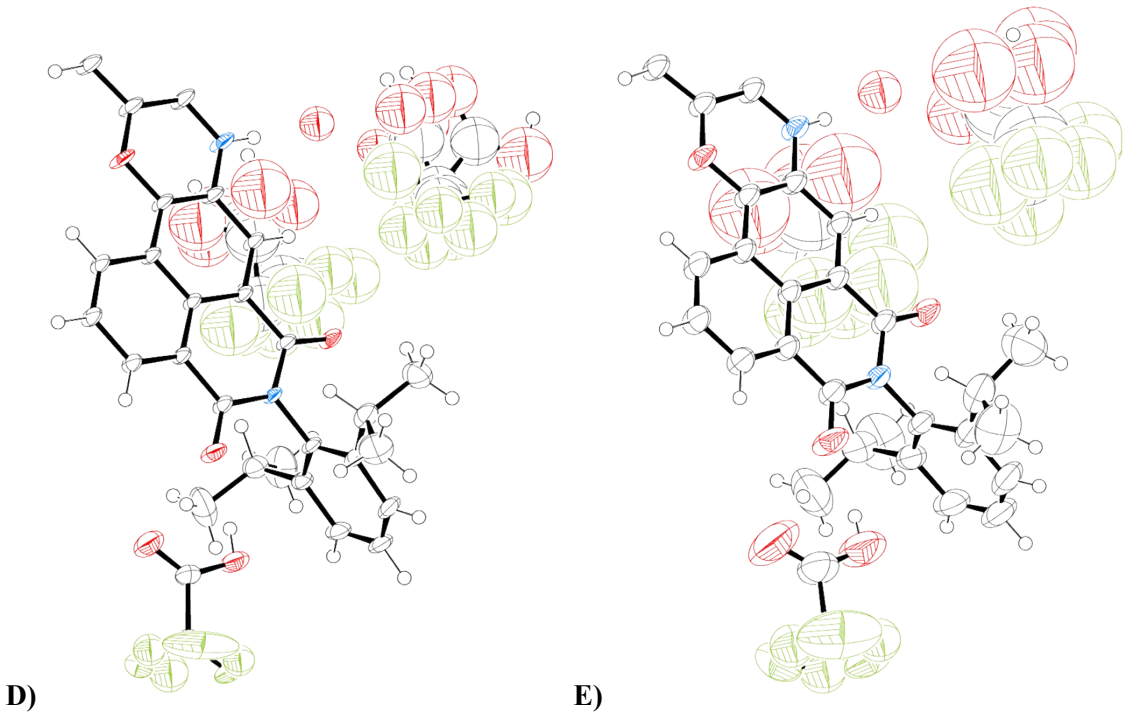

D)

E)

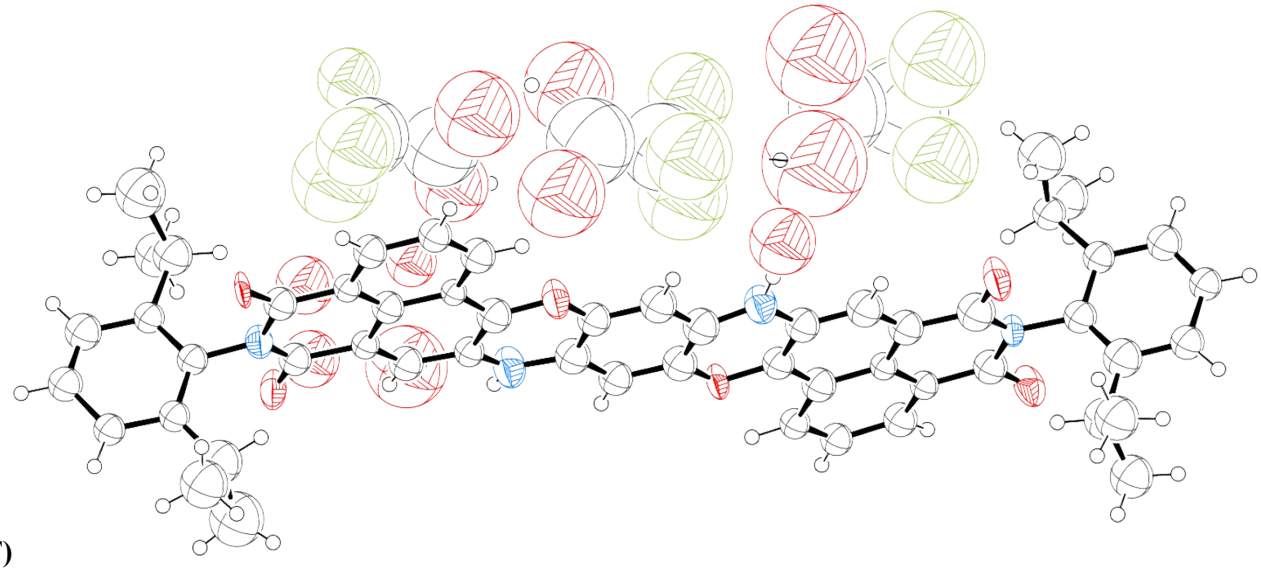

F)

Figure S44. Ellipsoids representation of asymmetric unit content (ASU) for (A) **1** at 100K, (B) **1** at 298K, (C) **1Br** at 100K, (D) **1•TFA** polymorph α at 100K, (E) **1•TFA** polymorph α at 298K and (F) **1•TFA** polymorph β at 100K (50% probability).

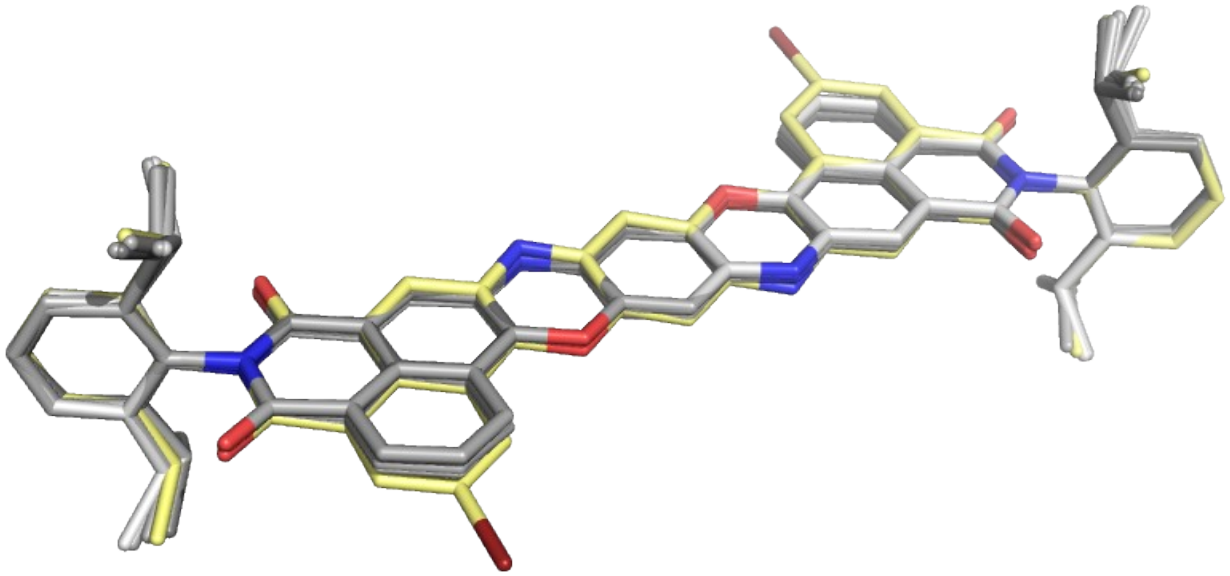

Figure S45. Overlap of crystallographically independent TPDO based NDI molecules, showing the equivalent conformations adopted (R.M.S.D. < 0.25 Å – brominated variant is represented with yellow sticks). Hydrogens omitted for clarity.

References

1 F. Vernuccio, R. Vanna, C. Ceconello, A. Bresci, F. Manetti, S. Sorrentino, S. Ghislanzoni, F. Lambertucci, O. Motiño, I. Martins, G. Kroemer, I. Bongarzone, G. Cerullo and D. Polli, *J. Phys. Chem. B*, 2023, **127**, 4733–4745.

2 C. H. Camp, Y. J. Lee and M. T. Cicerone, *J. Raman Spectrosc.*, 2016, **47**, 408–415.

3 N. F. Fedko and V. F. Anikin, *J. Org. Pharm. Chem.*, 2015, **13**, 12–15.

4 J. Réhault, M. Maiuri, A. Oriana and G. Cerullo, *Rev. Sci. Instrum.*, 2014, **85**, 1–11.

5 A. Lausi, M. Polentarutti, S. Onesti, J. R. Plaisier, E. Busetto, G. Bais, L. Barba, A. Cassetta, G. Campi, D. Lamba, A. Pifferi, S. C. Mande, D. D. Sarma, S. M. Sharma and G. Paolucci, *Eur. Phys. J. Plus*, 2015, **130**, 1–8.

6 J. P. Glusker, *Acta Crystallogr. Sect. D Biol. Crystallogr.*, 2010, **D66**, 125–132.

7 J. Agirre, M. Atanasova, H. Bagdonas, C. B. Ballard, A. Baslé, J. Beilsten-Edmands, R. J. Borges, D. G. Brown, J. J. Burgos-Mármol, J. M. Berrisford, P. S. Bond, I. Caballero, L. Catapano, G. Chojnowski, A. G. Cook, K. D. Cowtan, T. I. Croll, J. Debreczeni, N. E. Devenish, E. J. Dodson, T. R. Drevon, P. Emsley, G. Evans, P. R. Evans, M. Fando, J. Foadi, L. Fuentes-Montero, E. F. Garman, M. Gerstel, R. J. Gildea, K. Hatti, M. L. Hekkelman, P. Heuser, S. W. Hoh, M. A. Hough, H. T. Jenkins, E. Jiménez, R. P. Joosten, R. M. Keegan, N. Keep, E. B. Krissinel, P. Kolenko, O. Kovalevskiy, V. S. Lamzin, D. M. Lawson, A. A. Lebedev, A. G. W. Leslie, B. Lohkamp, F. Long,

M. Malý, A. J. McCoy, S. J. McNicholas, A. Medina, C. Millán, J. W. Murray, G. N. Murshudov, R. A. Nicholls, M. E. M. Noble, R. Oeffner, N. S. Pannu, J. M. Parkhurst, N. Pearce, J. Pereira, A. Perrakis, H. R. Powell, R. J. Read, D. J. Rigden, W. Rochira, M. Sammito, F. S. Rodríguez, G. M. Sheldrick, K. L. Shelley, F. Simkovic, A. J. Simpkin, P. Skubak, E. Sobolev, R. A. Steiner, K. Stevenson, I. Tews, J. M. H. Thomas, A. Thorn, J. T. Valls, V. Uski, I. Usón, A. Vagin, S. Velankar, M. Vollmar, H. Walden, D. Waterman, K. S. Wilson, M. D. Winn, G. Winter, M. Wojdyr and K. Yamashita, *Acta Crystallogr. Sect. D Struct. Biol.*, 2023, **79**, 449–461.

8 P. R. Evans and G. N. Murshudov, *Acta Crystallogr. Sect. D Biol. Crystallogr.*, 2013, **69**, 1204–1214.

9 G. M. Sheldrick, *Acta Crystallogr. Sect. A Found. Crystallogr.*, 2015, **71**, 3–8.

10 G. M. Sheldrick, *Acta Crystallogr. Sect. C Struct. Chem.*, 2015, **71**, 3–8.

11 P. Emsley, B. Lohkamp, W. G. Scott and K. Cowtan, *Acta Crystallogr. Sect. D Biol. Crystallogr.*, 2010, **66**, 486–501.

12 L. J. Farrugia, *J. Appl. Crystallogr.*, 2012, **45**, 849–854.

13 C. F. MacRae, I. Sovago, S. J. Cottrell, P. T. A. Galek, P. McCabe, E. Pidcock, M. Platings, G. P. Shields, J. S. Stevens, M. Towler and P. A. Wood, *J. Appl. Crystallogr.*, 2020, **53**, 226–235.

14 Schrodinger,. L., L., C., *PyMOL Molecular Graphics System*, 2015, 1, 8.